Characterization of age-related myelination deficits in a rat model for schizophrenia

Marigoula Vlassopoulou

Supervisors: Astrid Vallès Sanchez[1,2], Gerard J.M. Martens[1]

Affiliations:

1: Department of Molecular Animal Physiology, Donders Centre for Neuroscience, Radboud Institute for Molecular Life Sciences, Radboud University Nijmegen, The Netherlands

2: Department of Cognitive Neuroscience, Faculty of Psychology and Neurosciences, Maastricht University, The Netherlands

Corresponding author: Marigoula Vlassopoulou, mary.vlassopoulou@gmail.com

Abstract: Schizophrenia (SZ) is a debilitating neuropsychiatric disorder that affects millions of people around the world. A growing body of evidence points towards the involvement of hypomyelination of the prefrontal cortex (PFC) in the development of the cognitive symptoms of the disorder. Our hypothesis is that SZ patients exhibit elevated oxidative stress (i.e. redox imbalance) throughout the brain early in development and this disrupts the ongoing process of myelination in the late-maturing PFC, resulting in clinical manifestations of cognitive dysfunction. To tackle the neurophysiological underpinnings and postnatal developmental timing of such a mechanism, we combined molecular and cellular analysis in the apomorphine-susceptible (APO-SUS) rat model for schizophrenia, using APO-UNSUS rats as their control counterparts. First, we assessed the mRNA expression levels of genes related to myelin, oxidative stress and oligodendrocytes (OLs, the myelinating glia of the central nervous system) in the mPFC, striatum and corpus callosum of post-natal day (PND) 21 and PND28 male animals. Secondly, we used immunohistochemistry to assess differences in the percentage of OLs and their precursors in the mPFC, striatum, corpus callosum and hippocampus of PND21 and PND90 male rats, as well as the extent of myelination in axons of the mPFC and barrel cortex of these animals. The results showed that, while differential expression in redox-related genes is already present at PND21 in multiple brain regions, myelin- and OL-related molecular and cellular abnormalities are more prominent in animals aged PND28 and older, and occur specifically in the APO-SUS mPFC. The results of this study provide more insights into the neuropathology of SZ and clues for developing therapeutic approaches for the disorder.

Keywords: myelination; redox imbalance; oligodendrocytes; oligodendrocyte precursors; mPFC; APO-SUS; APO- UNSUS; mRNA expression; OLIG2; NG2; PLP

1. Introduction

1.1 Schizophrenia and cognitive function

Schizophrenia (SZ) is a severe and chronic mental disorder that afflicts approximately 1% of the world's population. The typical age of onset is late adolescence to early adulthood, with a tendency for earlier occurrence in males (National Institute of Mental Health, 2015). Clinical manifestations of the disorder display great heterogeneity, with its diverse symptomatology ranging from positive, i.e., delusions, hallucinations or disorganized speech, to negative symptoms, i.e., affective flattening, alogia (poverty of speech) or abolition (lack of motivation) (American Psychiatric Association, 1994). Another aspect of SZ that has a considerable impact on patients' well-being is the progressive emergence of neurocognitive dysfunction, with the most prominent deficits affecting attention, memory and executive functioning (Goldberg & Green, 1995; Reichenberg et al., 2009). Cognitive symptoms are not included in the diagnostic criteria for SZ because they are not discriminating of this particular disorder, however, it has been suggested that cognitive decline that is observed to precede psychosis could be used as an important predictor of the disease (Bora, 2009; Lewandowski et al., 2011; Tandon et al., 2013; Barch et al., 2013).

To this day, there are no pharmacological treatments targeting the negative and cognitive symptoms of SZ, and this is mainly due to the lack of understanding for the pathophysiology of the disorder. Current medications prescribed to schizophrenic patients are antipsychotic drugs that provide relief to the positive symptoms only (Minzenberg et al., 2014).

1.2 Implication of the prefrontal cortex in SZ pathogenesis

The association of SZ with cognitive dysfunction brings the prefrontal cortex (PFC) into the spotlight. The PFC has a central role in cognition, by being the region that integrates highly processed information from multiple brain areas to ultimately orchestrate our thoughts, actions and overall behavior (Miller et al., 2002). Consistent with this theory, numerous studies have shown that lesions in PFC early in life induce disturbances in cognitive function and behavior (Eslinger et al., 2004; Schneider & Koch, 2005).

One of the PFC's characteristic features is its relatively slow maturation process, which is not complete until early adulthood, an age that marks the refinement of cognitive functions, such as reasoning and executive functioning (Goldman-Rakic et al. 1997; Lewis 1997; Fuster, 2002; Andersen, 2003). This timing also coincides with the onset of SZ, suggesting that abnormalities in the developmental trajectory of the PFC could contribute to the neuropathology of the disorder. In support of this hypothesis, many studies have demonstrated a correlation between the distortion of these maturational processes and the emergence of SZ, leading to the hypothesis that SZ is a disorder of the cortex (reviews by Catts et al., 2013 and Woo, 2014).

1.3 Oligodendrocytes and myelination of PFC

In search of the etiology of such disturbances in PFC development, research in the brains of schizophrenic patients revealed hypofrontality as well as aberrant structural and functional connectivity, including deficits in the process of interest for the present study, namely myelination (Callicott et al., 2003; Tan et al., 2006; Potkin et al., 2009; Sakurai et al., 2015; Chen et al., 2016). Myelination is a long process which is developmentally regulated and it was classically thought to remain essentially static after young adulthood. However, recent data indicate that it keeps being dynamic throughout life and is influenced by neuronal activity (for a review see Haroutunian et al., 2014). Alterations in myelination are thought to play a key role not only in classic neurological disorders such as multiple sclerosis, but also in neuropsychiatric disorders like SZ (Davis et al., 2003).

In the central nervous system, the cells responsible for myelination are the oligodendrocytes (OLs) (Höistad et al., 2009). OLs encapsulate multiple adjacent neuronal axon segments with a myelin sheath that optimizes signal transmission by increasing its speed (Nave & Werner, 2014). Developmentally, OLs derive from subventricular zone progenitors that differentiate to oligodendrocyte precursor cells (OPCs). These cells migrate throughout the CNS and give rise to mature myelinating OLs (Emery, 2010). OPCs remain present in the adult brain and are ready to differentiate, as myelination is a process that continues in the adult life.

Apart from the aforementioned abnormalities in myelination as well as the observed dysregulation of myelin-related genes (Hakak et al., 2001; Flynn et al., 2003), studies in SZ have also revealed impairments at a cellular level. More specifically, there is evidence for decreased number and altered structure of OLs (Vartanian et al., 1999; Vostrikov & Uranova, 2011; Vikhreva et al., 2016), as well as impaired OPC differentiation (Monin et al., 2014; Mauney et al., 2015). The underlying mechanisms that lead to this OPC and OL dysfunction are not clarified yet, but one of the hypotheses that stand out suggests that oxidative stress is a critical causative factor, as OPCs are particularly vulnerable to it (Do et al., 2009; French et al., 2009).

1.4 Redox imbalance and myelination

Myelination is a carefully orchestrated process and that feature makes it vulnerable to alterations in the homeostasis of the brain. A case of impaired regulation that can lead to suboptimal myelination is oxidative stress, as OPC differentiation is sensitive to it (Butts et al., 2008; French et al., 2009; Monin et al., 2014). Oxidative stress occurs due to excessive accumulation of reactive oxygen species (ROS, by-products of chemical reactions) in the tissue (Reddy & Yao 1996; Yao et al., 2001; Do et al., 2009; Bitanihirwe & Woo, 2011). It emerges after overproduction of ROS or malfunction of the endogenous antioxidant defense system that is responsible for keeping the redox (chemical reduction-oxidation reaction) balanced (Woo, 2014). Redox imbalance is believed to be a causative factor in the pathophysiology of SZ, as many studies have found a significant correlation between oxidative stress and development of the disorder (Flatow et al., 2013; Monin et al., 2014).

An important antioxidant that is found to be deficient in SZ patients is glutathione (Do et al. 2009; Monin et al., 2014). Decreased levels of glutathione result in failure to keep redox balanced and ultimately may decrease OPC survival. This deficit might not be detrimental for brain regions like corpus callosum and striatum that mature early in development, but it could be crucial for PFC myelination that, as mentioned earlier, occurs later in life hence it remains exposed to the effects of glutathione dysregulation for an extended time window.

These observations lead to our hypothesis that exposure to oxidative stress early in life gives rise to aberrations in myelination of the late-maturing PFC, resulting in clinical manifestations of cognitive decline in SZ. If such a hypothesis is supported by our findings, it could potentially lead to the development of novel therapeutic approaches for SZ's cognitive symptoms that target at the control of oxidative stress and/or myelination. Subsequently, they could limit its deleterious effects on brain physiology and, ultimately, on behavior.

1.5 APO-SUS rats as a model for SZ

In order to study whether redox imbalance is involved in SZ pathophysiology through its effect on myelination, we used the APO-SUS/ APO-UNSUS rat model. This model has previously been developed with the use of neuropharmacological selective breeding by Ellenbroek & Cools (Ellenbroek *et al.*, 1995; Ellenbroek & Cools, 2000). Wistar rats were selectively bred with respect to the sensitivity of their behavioural phenotype to administration of apomorphine, a dopamine D2 receptor agonist. APO- SUS (apomorphine-susceptible) rats fall into the one extreme of the population distribution and exhibit many SZ-like features at different levels, ranging from abnormalities in information processing to an overactive dopaminergic system, compared to their phenotypic counterparts, APO-UNSUS (apomorphine-unsusceptible) (Ellenbroek et al., 1995; Ellenbroek & Cools, 2000, 2002; van der Elst et al., 2005). Most importantly, adult APO-SUS rats show a regional specific differential expression of many myelin-related genes that is similar to that of schizophrenic patients (Eijsink, V., Martens, G. et al., unpublished observations). So far, findings from mRNA quantification in male APO-SUS at multiple developmental time points ranging from postnatal day (PND) 60 to 12 months of age have revealed dysregulation of myelin-related genes specifically in the mPFC (Eijsink, V., Maas, D., Vallès-Sanchez, A., Martens, G. et al., unpublished data). However, redox-related genes were dysregulated not only there but also in other brain regions, including the striatum and corpus callosum. Interestingly, the results of this type of analysis at PND28 were inconclusive for myelin-related genes in mPFC, suggesting that these deficits might be starting to emerge at a proximal preceding age.

1.6 Objectives

Taking into account the above findings, the objective of the present study was to further characterize the myelination deficits that seem to be age-related in the APO-SUS / APO-UNSUS rat model and to investigate the potential role of cerebral oxidative stress in the

pathogenesis of SZ. For this purpose, a combination of molecular and cellular techniques was applied on brain tissue from male rats of different ages.

We examined in the regions of interest the relative mRNA expression profiles for genes related to myelin, OLs and redox. Firstly, the analysis at PND28 was repeated and subsequently it was extended at an earlier time point, namely PND21. The main research question to be answered here was whether alterations of myelin-related gene expression are age-dependent and if they indeed are, which is the developmental time point that marks their rise. According to the previous observations, we expected to find less prominent myelin deficits in mPFC of the younger APO-SUS group. Furthermore, we aimed to examine whether signs of redox dysregulation were already present early on in younger APO-SUS and possibly preceding myelin deficits. Lastly, we searched for alterations in OL-related gene expression and since analysis of older groups hasn't provided any evidence for such disturbances, we wouldn't expect to observe any in PND28 and PND21 either.

At a cellular level, the analysis involved immunohistochemistry with specific markers for cells that belong to the OL lineage, to measure the proportion of OPCs and mature OLs in APO-SUS and their counterparts APO-UNSUS. The markers were OLIG2 (oligodendrocyte lineage transcription factor 2), a protein expressed by the whole OL lineage and NG2 (neural/glial antigen 2) which is expressed only by OPCs. The goal of this investigation was to provide information on the density of OLs and their precursors in the brains of young adult rats (PND90) and to juxtapose the findings with those of PND21 animals, to clarify whether potential cellular alterations in APO-SUS rats already exist before early adolescence or occur gradually. Moreover, this analysis will shed light on the cause of potential mature OL deficits that can be attributed to either OPC differentiation or OPC proliferation.

As for the regions of interest, apart from PFC we also investigated corpus callosum and striatum as controls because they mature much earlier in development and we do not expect to observe any differences, as myelination will already be completed by the time oxidative stress takes place. Furthermore, we included the hippocampus due to indications from unpublished data of our lab that there are alterations in the myelination and OL density in this region of the APO-SUS line.

2. Materials and Methods

The experimental procedures of the present study were approved by the Animal Ethics Committee of the Radboud University Nijmegen, according to the Dutch legislation.

2.1 Animals

mRNA expression of the genes of interest was measured in 16 PND21 male rats and 16 PND28 male rats (APO-SUS n=8 and APO-UNSUS n=8 per age). The animals were housed with their mother and littermates and consumption of water and food (ssniff Spezialdiäten GmbH, Soest) was ad libitum. Room temperature was kept at 20-22℃,

humidity at 29-39%, light intensity at 80 lux and the light-dark circle followed a 12 hour paradigm.

Immunohistochemical analysis (IHC) was applied at two ages of male APO-SUS and APO-UNSUS rats, namely PND 21 (n=8 APO-SUS and n=8 APO-UNSUS) and PND90 (n=7 APO-SUS and n=7 APO- UNSUS). PND21 animals were housed with their mother and littermates, while PND90 animals were housed in pairs after weaning (PND28). In both housing types, conditions were the same with the ones described in above.

2.2 mRNA expression analysis

2.2.1 Brain cryosectioning and micropunching

Animals were sacrificed by direct decapitation without anaesthesia, under basal conditions. Brains were removed and immediately frozen in dry ice. They were stored at -80℃ and moved at -20℃ one day prior to cryosectioning. Brain tissue was cut in 300 μm thick sections with the use of a cryostat (Microm HM500 OM) at -20℃. Regions of interest (ROIs) included mPFC (prelimpbic and infralimbic), striatum and corpus callosum (representative images in Suppl. Fig. 1). mPFC and striatum were punched with microneedles (Harris Inc.) of 1.2μm and 3.0μm diameter respectively and corpus callosum was microdissected with a scalpel at room temperature. Each of them was collected from 6 consecutive sections, Bregma 3.70 to 2.20 mm for mPFC and Bregma 1.60 to -0.20 mm for striatum and corpus callosum. For PND28, striatum punches included both its dorsolateral and dorsomedial subregions, whereas in PND21 these two subregions were acquired separately with the use of a 1.2mm microneedle (Harris Inc.) and an extra region of interest was added, namely cingulate cortex (1.2mm microneedle, Harris Inc.). The collected tissue was placed in one 2mL Eppendorf tube per region and then stored at -80℃.

2.2.2 RNA isolation

Tissue samples were homogenized with the use of 1ml Trizol reagent and a stainless-steel bead per Eppendorf tube and shaking in a Tissue Lyser (Qiagen) at maximum speed for 2 minutes. Chloroform (200 μl) was added to divide the aqueous from the organic phase. The aqueous phase that contains the sample's RNA was removed and transferred in a new tube. RNA was then precipitated in pellets with the use of 20 μl glycogen and 400 μl isopropanol. The supernatant was removed and pellets were washed twice with 1ml ice-cold 75% ethanol. Pellets were then air-dried at room temperature for 10 minutes and dissolved in MilliQ water (30 μl for whole striatum, 20μl for corpus callosum and 15μl for PFC, dorsolateral striatum and dorsomedial striatum samples) through incubation at 55℃ for 10 minutes.

RNA concentration and purity in the samples was measured in a DS-11 FX spectrophotometer (Denovix). RNA quality was measured by electrophoresis in 1% agarose gel. The loading solution (1μl of the sample, 1μl of nuclease-free H2O, 2μl of RNA loading dye) was incubated for 10 minutes at 70℃ and after loading onto the agarose gel it was run at 100V for 30 min.

RNA samples were stored at -80℃ until further use.

2.2.3 cDNA synthesis

To quantify the relative expression of redox-, myelin- and OL-related mRNAs from the collected tissue samples, we used quantitative PCR (qPCR) analysis. The first step for this procedure is reverse transcription of RNA to double-stranded complementary DNA (cDNA).

Prior to cDNA synthesis, RNA samples were treated with DNase I (Fermentas) to remove any remaining traces of genomic DNA or DNA contamination. The created mix included 5 µl of total RNA solution, 1 µl DNase, 0.5 µl RNase A inhibitor (RNasin), 2 µl First Strand Buffer (5x FSB) and 1.5 µl MilliQ water. RNA solutions from PND28 tissue included 0.2415 µg of RNA from mPFC and 0.5 µg from striatum and corpus callosum samples. PND21 RNA samples contained 0.3 µg of RNA from prelimbic and infralimbic mPFC, 0.25 µg from cingulate mPFC, 0.5 µg from dorsolateral striatum, 0.3µg from dorsomedial striatum and 0.25 µg from corpus callosum. Mixes underwent incubation at 37℃ for 30 minutes and then at 75℃ for 5 minutes.

cDNA synthesis was based on Thermo Scientific Kit (Revert Aid H-minus first strand cDNA synthesis kit) instructions. It combined reverse transcription, a reaction catalyzed by the enzyme reverse transcriptase (RT) that transcribes RNA back to cDNA, and PCR, a method that amplifies cDNA templates and allows detection of small amounts of this nucleic acid. cDNA was then diluted in MilliQ water and stored at -20℃ until further processing.

Two controls for the purity of the samples were added. One that did not include reverse transcriptase and a second that did not include any RNA from the samples. In both cases, signal detection would indicate contamination at some point of the procedure.

2.2.4 qPCR

The mix for qPCR included 2.0 µl cDNA, 0.8 µL 5 µM forward primer, 0.8 µL 5 µM reverse primer, 5 µL SybrGreen mix (containing dNTPs, thermostable hot-start DNA polymerase and SYBR Green dye) and 1.8 µL MilliQ water. The primer pairs targeted 4 housekeeping genes, 2 redox-related genes, 7 myelin-related genes, 2 OL transcription factors, an OPC marker (for PND21 only) and an astrocyte marker (see Supplemental Table 1 for primer sequences). Housekeeping genes were used to extract a normalization factor, using GeNorm (Vandesompele et al., 2002), and subsequently measure the relative expression of every gene of interest per animal.

This mix was pipetted for every sample by a robot (Corbett Robotics) and qPCR was performed with the Rotor Gene 6000 Series (Corbett Life Sciences).

2.2.5 Statistics

Statistical analysis was performed with the program IBM SPSS Statistics version 23.0. The mean normalized mRNA expression was compared between APO-SUS and APO-UNSUS samples. Furthermore, we compared PND21 and PND28 APO-SUS samples' difference in RNA expression from the average expression of their APO-UNSUS counterparts. Outliers were removed with the Grubbs test for outliers and statistical

significance was determined by the independent samples Student's t-test with a significance level of $p \leq 0.05$. Graphs were created with the program GraphPad Prism 7.

2.3 Immunohistochemical analysis

2.3.1 Tissue fixation

PND90 animals were anaesthetized by an intraperitoneal injection of sodium pentobarbital (90 mg/kg) and then perfused transcardially, first with 1xPBS (Phosphate Buffered Saline, approx. 100 ml) and then with 2% paraformaldehyde (PFA) in 1xPBS (approximately 300 ml, pH 7.5). Both solutions were ice-cold. When the perfusion procedure was completed, brains were extracted from the skull and immersed in 50 ml of 2% PFA in 1xPBS at 4℃ for 1 hour. PND21 animals were sacrificed by direct decapitation without anesthesia, after which the brains were extracted and post-fixated by immersion in 2% PFA in 1xPBS for 48 hours at 4℃. Subsequently, brains were transferred in sucrose for cryoprotection (30% sucrose in 1xPBS for 2-3 days at 4℃, until they were sunk at the bottom of the tube), then frozen on dry ice, stored at -80℃ and moved to -20℃ one day prior to sectioning.

2.3.2 Tissue sectioning and staining

The right hemisphere of every brain was sectioned coronally with the use of a cryostat (Microm HM500 OM) at -25℃. The left hemispheres were kept for other analyses. Ten μm thick sections were serially cut from all regions of interest. The subsequently analyzed sections were collected in 20 series from the following depths of the brain, as measured by millimeters from Bregma: 4 sections from 3.20mm to 2.20mm for mPFC, 1 section at 1.60mm and another at 0.70mm for striatum and corpus callosum, 1 section at -3.14 and a second section at -3.80 for hippocampus and barrel cortex. All sections were directly mounted on Superfrost plus glass slides (Thermo Scientific) and stored at -20℃ until further processing for immunostaining.

The primary aim of this experiment was to measure the total number of cells that belong to the OL lineage, as well as the number of OPCs and mature OLs separately in the ROIs. To achieve this, a 3-day sequential protocol was followed to perform a double staining for OLIG2 and NG2 (see Supplemental Table 2 for antibodies).

Thirty minutes before the start of IHC, the slides that carried the brain sections were transferred to room temperature until they were dry and a PAP pen was used to draw hydrophobic barriers around the sections. Then, slides were washed 2 times for 8 minutes. The washing buffer was 1xPBS containing 0.005% Tween and all the washes of this protocol were conducted on a moving plate. Slides were incubated in blocking buffer (5% NGS/NDS/NHS, 1% BSA, 1% glycine, 0.1% lysine, 0.4% triton X-100) for 1 hour, followed by an overnight incubation in OLIG2 primary antibody solution (1:400 in blocking buffer). On the second day of the procedure, slides were washed three times for 10 minutes and then incubated for 2 hours with the secondary antibody solution (Alexa fluor 555 goat anti-rabbit, 1:500 in blocking buffer). Three more 10-minute washes followed, then an incubation for 1

hour in blocking buffer to improve antibodies' sensitivity and an overnight incubation with the second primary antibody solution containing anti-NG2 (1:200 in blocking buffer). On the last day, slides were washed three times and incubated for 2 hours in the 2nd secondary antibody solution (Alexa fluor 488 goat anti-mouse, 1:500 in blocking buffer). Then, they were washed again three times for 10 minutes and incubated in Hoechst dye solution (1:100 in 1XPBS) for 30 minutes. Hoechst is a nucleic acid stain that binds to dsDNA, therefore it stains all cells and can serve as a reference for the anatomical configuration of the brain sections. After three last 10-minute washes, slides were coverslipped with Fluorsafe reagent (CalBioChem).

All steps were carried out at room temperature, incubations were performed in humidity chambers and after coverslipping, slides were stored at 4℃.

Additionally, another set of slides with tissue from PND90 animals only was stained with an antibody that targets PLP (myelin proteolipid protein). PLP is a protein located in the myelin sheath, therefore this staining results in visualization of myelinated axons. The IHC protocol followed for this purpose was the same as the one described above, but this time it lasted 2 days because it was a single staining with only one set of primary (anti-PLP, 1:200 in blocking buffer) and secondary (Alexa fluor 488 goat anti-mouse, 1:500 in blocking buffer) antibodies (see Supplemental Table 2 for antibodies' details). Conditions (temperature, incubation times, washes etc.) and the solutions used remained the same.

2.3.3 Image acquisition and analysis

The stained brain sections were imaged with the use of a Leica DM microscope and the program Leica GW4000 CytoFISH. The ROIs for OLIG2 and NG2 were a) mPFC, divided in its three subregions, cingulate, infralimbic and prelimbic, b) lateral and medial striatum, c) corpus callosum and d) hippocampus (see Suppl. Fig. 2). PLP expression was examined in the three aforementioned subregions of mPFC, as well as in barrel cortex. The objective lens used for the imaging was 20x for the OLIG2-NG2 combination, and 10x for PLP. Single images were acquired from all ROIs except for mPFC, that required multiple to cover the whole area. mPFC images were stitched with the program Adobe Photoshop CC 2015.

The counting of OLIG2- and NG2-positive cells was done by hand in Photoshop. The bins used in every ROI are illustrated in Supplemental Figure 2. Cells were counted as NG2-positive only if they were also OLIG2-positive.

For PLP analysis, we assessed the area covered by axons that were giving signal and hence expressed PLP. Images were inserted in FIJI and signal-to-noise ratio was ameliorated with the option "Subtract background", using a rolling ball radius of 50 pixels. Then, a threshold of 25/255 was applied to convert the images to a binary scale and the area limited to this threshold was measured.

2.3.4 Statistics

Statistical analysis was performed with the program IBM SPSS Statistics version 23.0. Comparisons were made between APO-SUS and APO-UNSUS on a) the total number of $OLIG2^+$ cells (whole OL lineage) b) the number of these cells that were also $NG2^+$ (OPCs) c) the number of $OLIG2^+$ that were $NG2^-$ (mature myelinating OLs) and d) the ratio of $NG2^+$ to $NG2^-$ cells (OPCs/OLs). Statistical significance was determined by the independent samples Student's t-test, using a significance level of $p \leq 0.05$. Outliers were removed with the Grubbs test for outliers and graphs were created with the program GraphPad Prism 7.

3. Results

3.1 mRNA expression analysis in mPFC, corpus callosum and striatum of PND21 and PND28 APO-SUS and APO-UNSUS rats

qPCR analysis of mRNA expression of selected genes was performed in mPFC, corpus callosum and striatum of APO-SUS and APO-UNSUS male rats, at the ages PND21 and PND28. We tested genes that fall into three categories, namely redox-, myelin- and OL-related, selected on the basis of previous studies from our group (Eijsink, V., Maas, D. et al., unpublished data).

3.1.1 mRNA expression in the mPFC of APO-SUS and APO-UNSUS rats

Redox-related genes

The redox-related genes examined were glutathione S-transferase mu 4 (Gstm4) and Peroxiredoxin 6 (Prdx6), two key enzymes of the glutathione metabolism pathway (Pastore et al., 2003; Fisher, 2010). Prdx6 showed a highly significant downregulation ($p \leq 0.001$) in the prelimbic and infralimbic cortices of APO-SUS animals in comparison to their control APO-UNSUS counterparts, both at PND21 and PND28 (Fig. 1A,B). On the contrary, Gstm4 was highly significantly upregulated in the prelimbic and infralimbic cortices of PND28 APO-SUS only ($p \leq 0.01$). mRNA expression in the cingulate cortex of PND21 rats showed the same pattern of Prdx6 downregulation and Gstm4 upregulation in APO-SUS ($p \leq 0.001$) (Fig. 1C).

Myelin-related genes

The myelin-related genes of interest were proteolipid protein 1 (Plp1), myelin associated glycoprotein (Mag), myelin basic protein (Mbp), myelin-associated oligodendrocyte basic protein (Mobp), claudin 11 (Cldn11), myelin oligodendrocyte glycoprotein (Mog) and oligodendrocytic myelin paranodal and inner loop protein (Opalin). qPCR analysis in prelimbic and infralimbic samples of PND28 animals revealed a highly significant downregulation in APO-SUS in all the tested genes, following the pattern that was previously seen in older ages (Fig. 2B) ($p \leq 0.01$ for Plp1, $p \leq 0.001$ for the rest of the genes). However, the case was not the same for these mPFC subregions at PND21. Only four of the genes were significantly downregulated in APO-SUS [Mag ($p \leq 0.001$), Plp1 ($p \leq 0.01$), Mobp

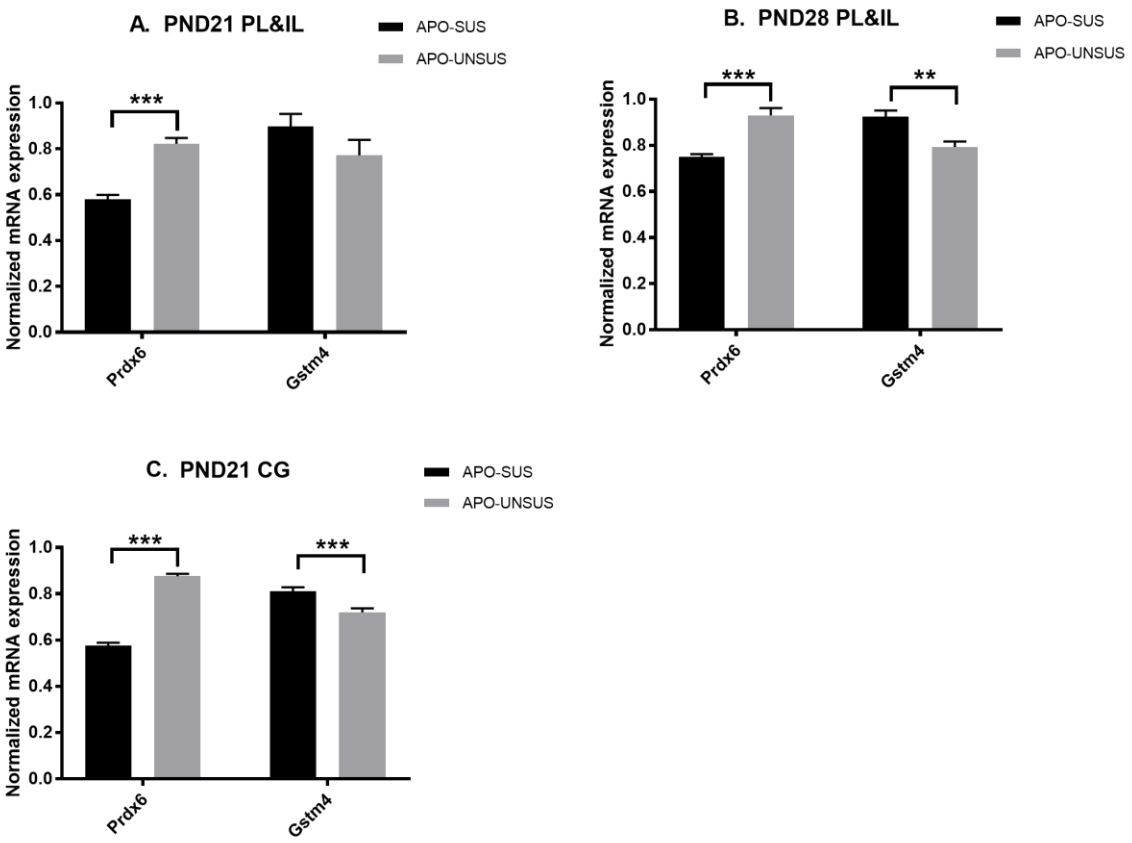

Figure 1. mRNA expression of redox-related genes in mPFC of APO-SUS and APO-UNSUS rats at PND21 and PND28

The bars represent the mean normalized mRNA expression of Prdx6 and Gstm4 in APO-SUS (black) and APO-UNSUS (grey) rats, along with error bars for the standard error of the mean. Asterisks (*) indicate statistically significant difference in gene expression between APO-SUS and APO-UNSUS, which was determined by the independent samples Student's t-test after removal of the outliers by the Grubbs test for outliers. Two asterisks (**) indicate $p \leq 0.01$ and three asterisks (***) $p \leq 0.001$. **A**. Normalised redox-related gene expression in prelimbic and infralimbic cortices of PND21 APO-SUS and APO-UNSUS rats (n=8 per group). Samples were normalized against the housekeeping genes Gapdh and Ywhaz. **B**. Normalized redox-related gene expression in prelimbic and infralimbic cortices of PND28 APO-SUS and APO-UNSUS rats (n=8 per group). Samples were normalized against the housekeeping genes β-Actin and Cyc-A. **C**. Normalized redox-related gene expression in cingulate cortex of PND21 APO-SUS and APO-UNSUS rats (n=7-8 per group). Samples were normalized against the housekeeping genes β-actin and Ywhaz.

($p \leq 0.05$) and Mog ($p \leq 0.05$)] and we also observed a trend for downregulation of Mbp ($p=0.08$) and Cldn11 ($p=0.051$) in this group (Fig. 2A).

The next aim was to make comparisons between these two ages, PND21 and PND28, at the level of myelin-related mRNA expression in prelimbic and infralimbic cortices. For this purpose, we calculated the percentage of expression decrease per gene in APO-SUS samples, using the average normalized expression of their APO-UNSUS control group as reference. As illustrated in Fig. 2D, PND28 APO-SUS demonstrated significantly greater

decrease in expression than PND21 APO-SUS in Mbp ($p \leq 0.001$), Mobp ($p \leq 0.01$), Mog ($p \leq 0.05$) and Opalin ($p \leq 0.05$), while Plp1 reached a trend towards significance ($p = 0.062$).

Finally, analysis of myelin-related gene expression in cingulate cortex of PND21 APO-SUS and APO-UNSUS animals revealed a significant downregulation of only one of the tested genes in APO-SUS, namely Cldn11 ($p \leq 0.05$) (Fig. 2C).

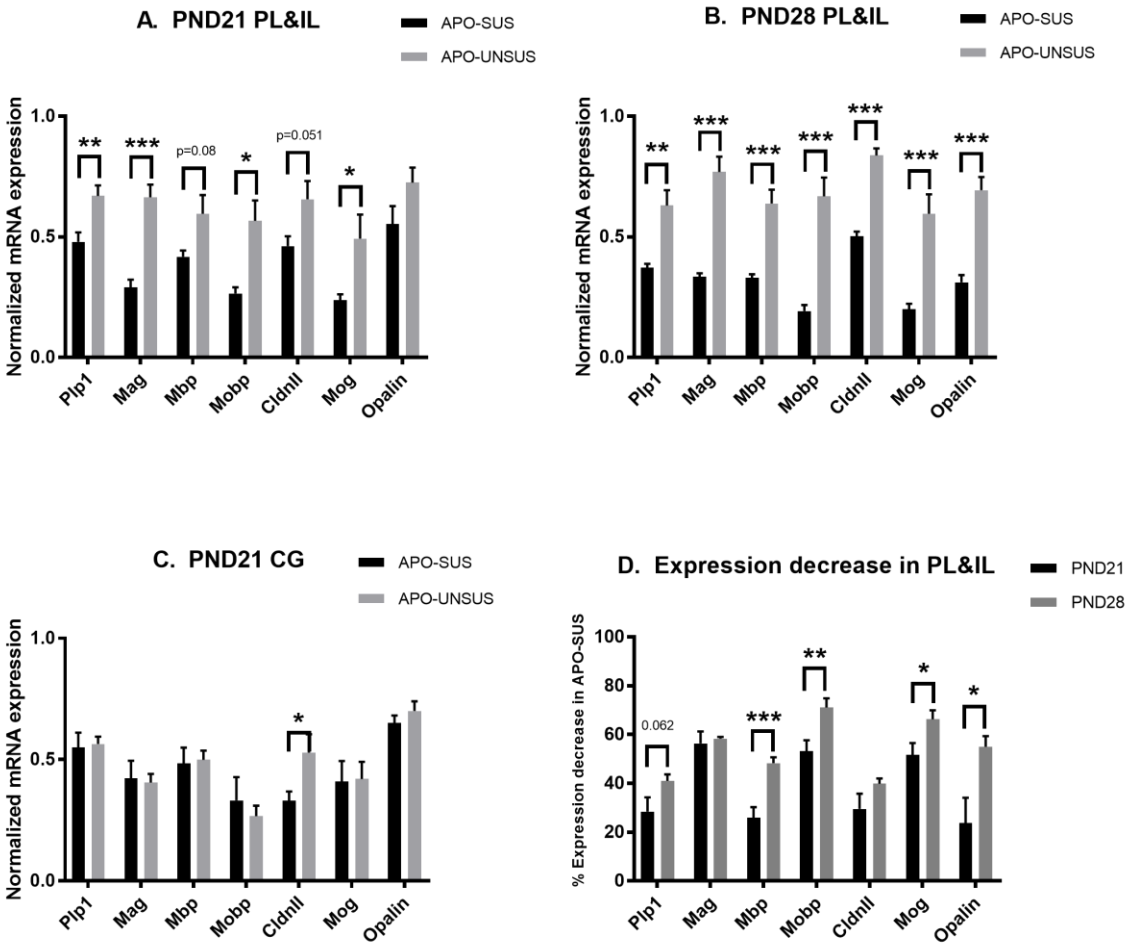

Figure 2. mRNA expression of myelin-related genes in mPFC of PND21 and PND28 APO-SUS and APO-UNSUS rats

Asterisks indicate statistically significant difference in gene expression between groups (* $p \leq 0.05$, ** $p \leq 0.01$, *** $p \leq 0.001$), which was determined by the independent samples Student's t-test, after removal of the outliers by the Grubbs test for outliers. **A-C.** The bars represent the mean normalised mRNA expression in APO-SUS (black) and APO-UNSUS (grey), along with error bars representing the standard error of the mean, for the genes Plp1, Mag, Mbp, Mobp, Cldn11, Mog and Opalin. **A**. Normalised expression levels in prelimbic and infralimbic cortices of PND21 animals (n=6-8 per group). Samples were normalized against the housekeeping genes β-Actin and Cyc-A. **B**. Normalised expression levels in prelimbic and infralimbic cortices of PND28 animals (n=7-8 per group). Samples were normalized against the housekeeping genes Gapdh and Ywhaz. **C**. Normalised expression levels in cingulate cortex of PND21 animals (n=7-8 per group). Samples were normalized against the housekeeping genes β-actin and Ywhaz. **D.** Percentage of decrease in normalised myelin-related expression of APO-SUS samples, compared to their APO-UNSUS control group. Black bars represent PND21 and grey bars PND28 (n=6-8 per group).

OL-related genes

mRNA expression in the mPFC of APO-SUS and APO-UNSUS rats was also assessed for the OL-related genes Sox10, Olig2 and PdgfaR. qPCR analysis showed, both at PND21 and at PND28, no significant differences in mRNA expression of these genes in the prelimbic and infralimbic cortices. However, normalized expression of Olig2 in cingulate cortex was significantly decreased ($p \leq 0.05$) in PND21 APO-SUS rats (Suppl. Fig. 3).

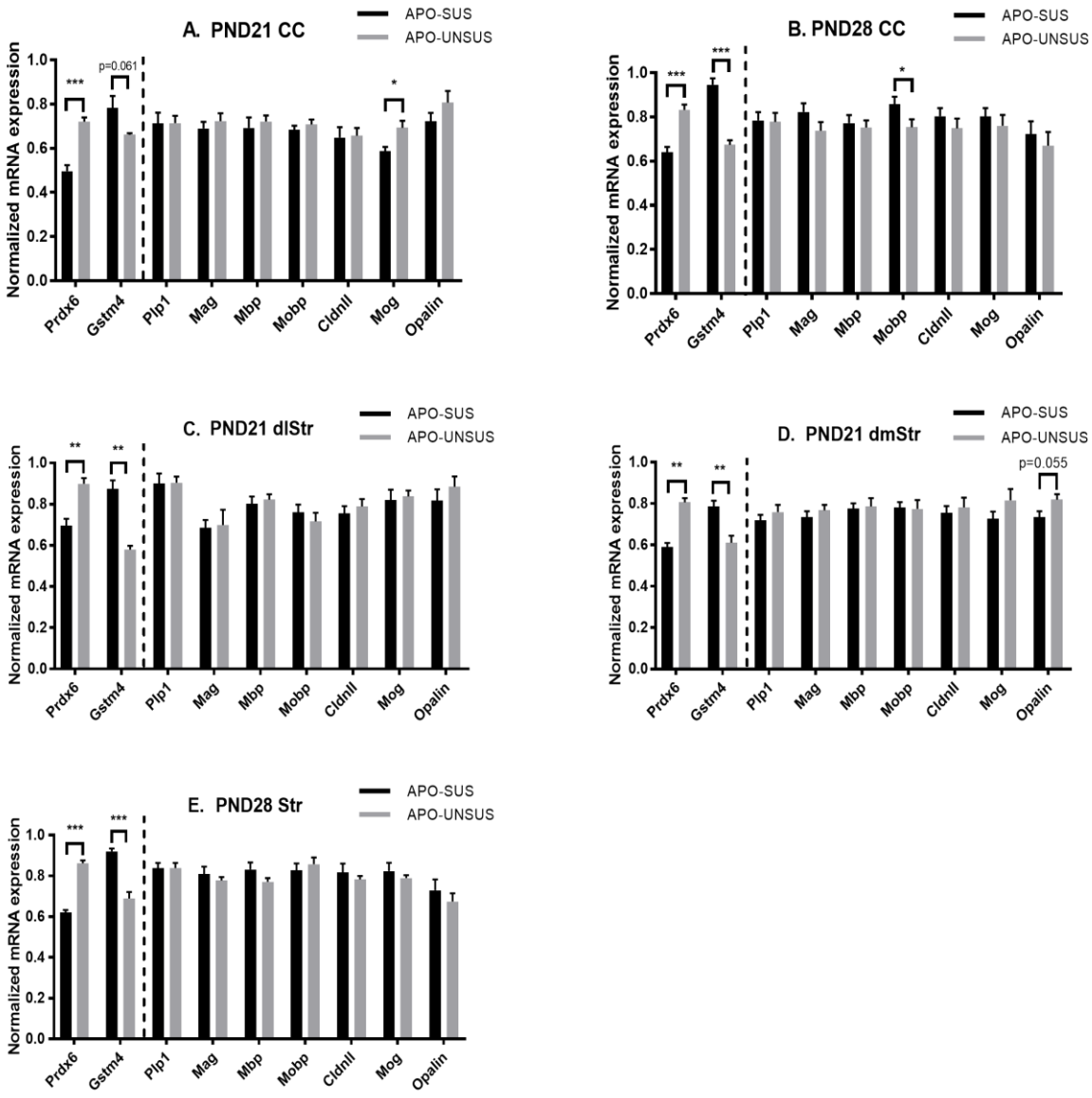

Figure 3. mRNA expression of redox- and myelin-related genes in corpus callosum and striatum of PND21 and PND28 APO-SUS and APO-UNSUS rats

The bars represent the mean normalised mRNA expression of redox-related (Prdx6 and Gstm4) and myelin-related (Plp1, Mag, Mbp, Mobp, Cldn11, Mog and Opalin) genes in APO-SUS (black) and APO-UNSUS (grey), along with error bars for the standard error of the mean. Asterisks (*) indicate statistically significant difference in gene expression between APO-SUS and APO-UNSUS, which was determined by the independent samples Student's t-test after removal of the outliers by the Grubbs test for outliers (* $p \leq 0.05$, ** $p \leq 0.01$, ***

p≤0.001). **A**. Mean normalized mRNA expression in corpus callosum of PND21 APO-SUS and APO-UNSUS rats (n=7-8 per group). Samples were normalized against the housekeeping genes β-Actin and Cyc-A. **B**. Mean normalized mRNA expression in corpus callosum of PND28 APO-SUS and APO-UNSUS rats (n=8 per group). Samples were normalized against the housekeeping genes Cyc-A and Ywhaz. **C**. Mean normalised mRNA expression in dorsolateral striatum of PND21 APO-SUS and APO-UNSUS rats (n=7-8 per group). Samples were normalized against the housekeeping genes β-actin and Gapdh. **D.** Mean normalised mRNA expression in dorsomedial striatum of PND21 APO-SUS and APO-UNSUS rats (n=7-8 per group). Samples were normalized against the housekeeping genes β-Actin and Ywhaz. **E.** Mean normalised mRNA expression in striatum of PND28 APO-SUS and APO-UNSUS rats (n=8 per group). Samples were normalized against the housekeeping genes β-Actin and Cyc-A.

3.1.2 mRNA expression in corpus callosum and striatum of APO-SUS and APO-UNSUS rats

mRNA expression for all genes that were examined in the mPFC subregions of PND21 and PND28 APO-SUS and APO-UNSUS rats was also analyzed in two early-maturing brain areas, the striatum and the myelin-rich corpus callosum. Redox-related genes showed highly significant differential expression between APO-SUS and APO-UNSUS in both ages and regions ($p \leq 0.01$) (Fig. 3A-E). The only exception was the expression of Gstm4 in the corpus callosum of PND21, although it had a trend (p=0.061) for the expected upregulation in APO-SUS (Fig. 3A).

Myelin-related genes, on the contrary, did not demonstrate the downregulation that was particularly prominent in the mPFC of PND28 APO-SUS and also seen, although to a lesser extent, in the prelimbic and infralimbic cortices of PND21 APO-SUS (Fig. 3A-E).

Finally, qPCR analysis of the OL-related genes Sox10, Olig2 and PdgfaR in corpus callosum and striatum showed no significant mRNA expression differences between APO-SUS and their APO-UNSUS counterparts ($p \geq 0.05$) and this finding was consistent for both ages, PND21 and PND28 (Suppl. Fig. 4A-E).

3.2 Immunohistochemical analysis of APO-SUS and APO-UNSUS rats

Immunohistochemistry was used for the assessment of OPC and OL density in multiple brain regions, as well as for the quantification of the protein PLP in the myelin sheaths of brain tissue from APO-SUS and APO-UNSUS rats.

3.2.1 OPC and OL quantification in PND21 and PND90 animals

The cellular approach of the present study involved the measurement of OPCs and OLs in brain tissue of PND21 and PND90 APO-SUS and APO-UNSUS male rats. The regions of interest are illustrated in Supplemental Figure 2. A representative image of the staining's outcome is provided at Fig. 4A.

OL and OPC quantification in the mPFC

Cell quantification in the infralimbic cortex of PND90 animals revealed that APO-SUS had a statistically significant decrease in OL density in comparison to their APO-UNSUS counterparts ($p \leq 0.01$), which was also reflected in the total number of cells that

belong to the oligodendrocyte lineage ($p \leq 0.05$) (Fig. 4C). The number of OPCs however, did not differ significantly between the two groups, although there was a trend for lower density in APO-SUS ($p=0.07$). The same pattern of decrease exclusively in OL density of APO-SUS was observed in the other two tested mPFC subregions of PND90 animals, the prelimbic ($p \leq 0.001$) and cingulate ($p \leq 0.05$) cortices (Suppl. Fig. 6B,D).

In PND21 animals however, this deviation of APO-SUS from their control counterparts in terms of OL density was not seen (Fig. 4B; Suppl. Fig. 6A,C). The only

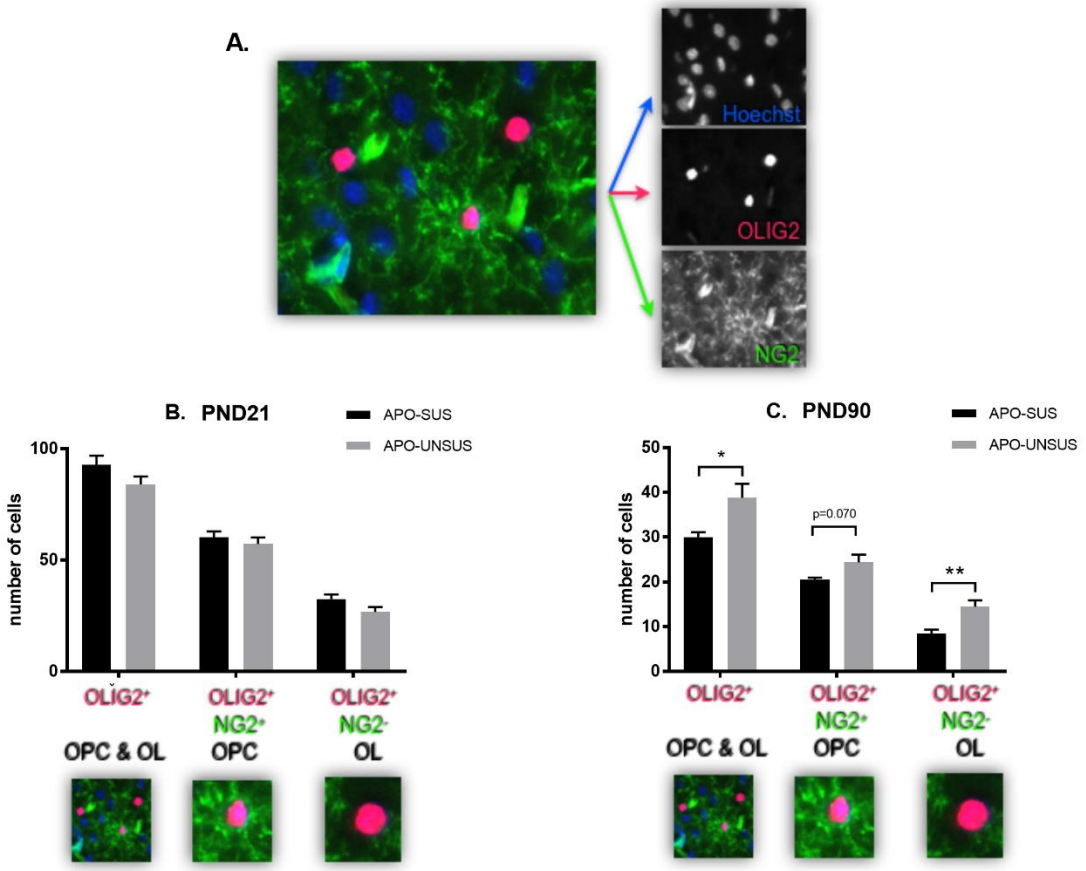

Figure 4. OPC and OL density in the infralimbic subregion of mPFC of APO-SUS and APO-UNSUS rats at PND21 and PND90

A. Representative image of the immunohistochemistry outcome. Blue colour represents the nucleic acid stain Hoechst, that marks all cells. Cells positive to OLIG2 (both OPCs and OLs) are colored dark pink. Green color indicates NG2 staining and the only cells from the OL lineage that are $NG2^+$ are the OPCs. **B-C**. Quantification of OPCs and OLs in the infralimbic cortex of PND21 (**B**, n= 7-8 per group) and PND90 (**C**, n= 6-7 per group) APO-SUS and APO-UNSUS male rats. The bars represent the mean number of cells in APO-SUS (black) and APO-UNSUS (grey), along with error bars for the standard error of the mean. Asterisks (*) indicate statistically significant difference in cell density between APO-SUS and APO-UNSUS, which was determined by the independent samples Student's t-test after removal of the outliers by the Grubbs test for outliers (* $p \leq 0.05$, ** $p \leq 0.01$). The first set of bars in each graph displays the number of $OLIG2^+$ cells, which is translated to the total amount of OLs and OPCs. This number was split in two in the next two sets of bars with the help of NG2 staining. The middle set depicts the number of OPCs alone (cells that are $OLIG2^+$ and $NG2^+$) and the last set of bars shows the number of mature OLs (cells that are $OLIG2^+$ but $NG2^-$).

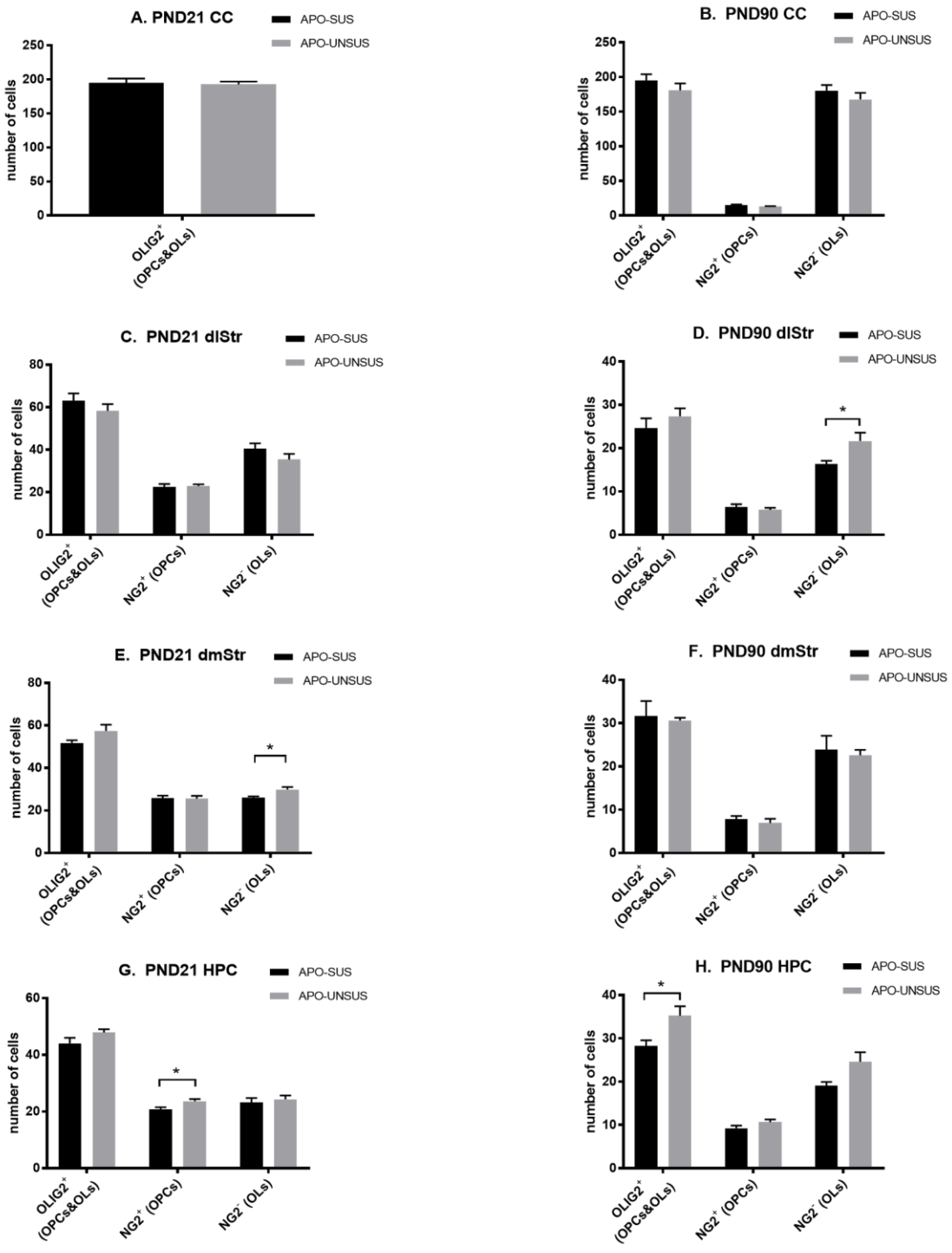

Figure 5. OPC and OL density in corpus callosum, striatum and hippocampus of APO-SUS and APO-UNSUS rats

Quantification of OPCs and OLs in other regions of interest in PND21 and PND90 APO-SUS and APO-UNSUS male rats. The bars represent the mean number of cells in APO-SUS (black) and APO-UNSUS (grey), along with error bars for the standard error of the mean. The asterisk (*) indicates statistically significant difference in cell density between APO-SUS and APO-UNSUS, which was determined by the independent

samples Student's t-test after removal of the outliers by the Grubbs test for outliers ($p \leq 0.05$). The first set of bars in each graph displays the number of $OLIG2^+$ cells, which is translated to the total amount of OLs and OPCs. This number was split in two in the next two sets of bars with the help of NG2 staining. The middle set depicts the number of OPCs alone (cells that are $OLIG2^+$ and simultaneously $NG2^+$) and the last set of bars shows the number of OLs (cells that are $OLIG2^+$ but $NG2^-$). **A**. OL density in the corpus callosum (CC) of PND21 APO-SUS and APO-UNSUS (n=8 per group). OPC density could not be determined due to the very high intensity of NG2 staining in this area. **B**. OPC and OL density in the CC of PND90 APO-SUS and APO-UNSUS (n=7 per group). **C**. OPC and OL density in the dorsolateral striatum (dlStr) of PND21 APO-SUS and APO-UNSUS (n=8 per group). **D**. OPC and OL density in the dlStr of PND90 APO-SUS and APO-UNSUS (n=6-7 per group). **E**. OPC and OL density in the dorsolateral striatum (dmStr) of PND21 APO-SUS and APO-UNSUS (n=7-8 per group). **F**. OPC and OL density in the dmStr of PND90 APO-SUS and APO-UNSUS (n=6-7 per group). **G**. OPC and OL density in the hippocampus (HPC) of PND21 APO-SUS and APO-UNSUS (n=8 per group). **H**. OPC and OL density in the HPC of PND90 APO-SUS and APO-UNSUS (n=7 per group).

exception was observed in OPCs of the prelimbic cortex, which were increased in APO-SUS ($p \leq 0.05$, Suppl. Fig. 6A).

OL and OPC quantification in corpus callosum, striatum and hippocampus

In corpus callosum, OL density measurement showed no significant differences between APO-SUS and APO-UNSUS at PND21 and PND90 (Fig. 5A,B). Similarly, OPC quantification at PND90 did not reveal any differences. Likewise, no OPC number deviations in APO-SUS were observed in the two examined subregions of striatum (dorsolateral and dorsomedial), both at PND21 and at PND90 (Fig. 5C-F). OL assessment however, demonstrated decreased density in dorsolateral striatum of PND90 APO-SUS (Fig. 5D), while in dorsomedial striatum, OLs where found to be significantly less in the younger (PND21) APO-SUS only (Fig. 5E). As for the hippocampus, OL density was not different between APO-SUS and their control counterparts both at PND21 and at PND90 (Fig. 5G-H). OPC number was also similar in SUS and UNSUS in the older groups (PND90), although the total number of OPCs and OLs were significantly lower in APO-SUS (Fig. 5H). Moreover, PND21 APO-SUS rats had significantly less OPCs than APO-UNSUS in their hippocampi (Fig. 5G).

OPC/OL ratio

The calculation of the OPC-to-OL ratio was performed to allow us to make more direct comparisons between the two tested ages per each region of interest. Starting with the mPFC, the results of this analysis showed that this ratio was significantly higher in the prelimbic and infralimbic cortex of APO-SUS rats only at PND90, but not at PND21 (Fig. 6). In the rest of the regions, the ratio was found to be significantly higher in the dorsolateral striatum of PND90 APO-SUS (Fig. 6B), while at PND21, OPC/OL ratio was significantly different only in the dorsolateral striatum (Fig. 6A).

Furthermore, OPC/OL ratio in mPFC is observably higher when compared to the rest of the examined regions, especially prelimbic and infralimbic cortices of PND90 animals.

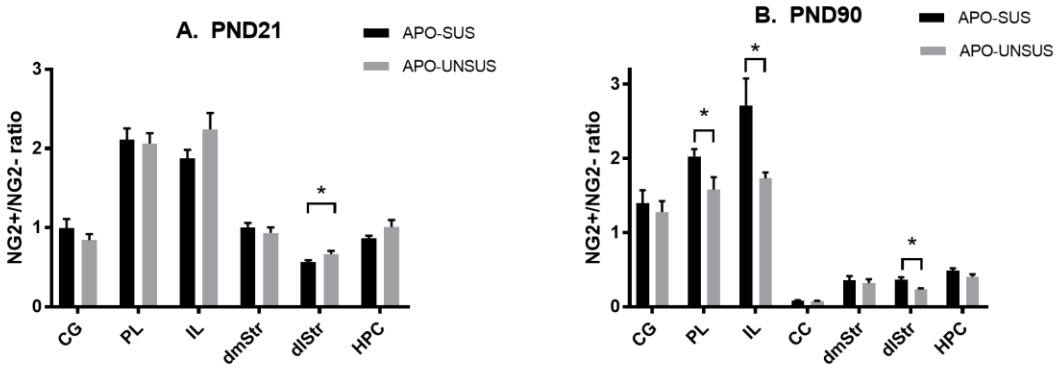

Figure 6. OPC /OL ratio in PND21 and PND90 APO-SUS and APO-UNSUS rats
The bars represent the mean OPC/OL ratio in APO-SUS (black) and APO-UNSUS (grey) male rats, as measured in the 3 subregions of mPFC [cingulate (CG), infralimbic (IL) and prelimbic (PL)], the corpus callosum (CC), dorsomedial (dmStr) and dorsolateral (dlStr) striatum and the hippocampus (HPC). Error bars indicate the standard error of the mean. The asterisk (*) indicates statistically significant difference in cell density between APO-SUS and APO-UNSUS, which was determined by the independent samples Student's t-test after removal of the outliers by the Grubbs test for outliers ($p \leq 0.05$). **A**. OPC/OL ratio at PND21 APO-SUS and APO-UNSUS (n=7-8 per group). **B**. OPC/OL ratio at PND90 APO-SUS and APO-UNSUS (n=6-7 per group).

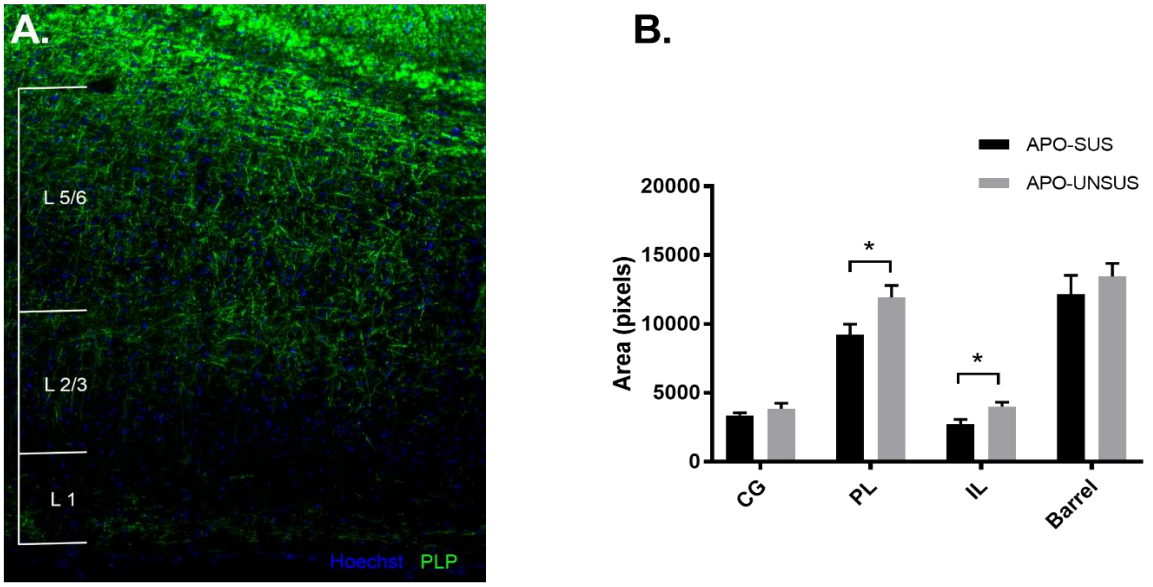

Figure 7. PLP quantification in PND90 APO-SUS/APO-UNSUS rats
A. Representative image of the immunohistochemistry outcome in the prelimbic cortex. Green colour indicates PLP staining and blue colour represents the nucleic acid stain Hoechst that marks all cells. **B**. Quantification of PLP in the cingulate (CG), infralimbic (IL), prelimbic (PL) and barrel cortices of PND90 APO-SUS and APO-UNSUS male rats (n=6-7 per group). The bars represent the mean covered area in APO-SUS (black) and APO-UNSUS (grey), along with error bars for the standard error of the mean. The asterisk (*) indicates statistically significant difference PLP coverage between APO-SUS and APO-UNSUS, which was determined by the independent samples Student's t-test after removal of the outliers by the Grubbs test for outliers ($p \leq 0.05$).

3.2.2 PLP quantification in PND90 APO-SUS and APO-UNSUS rats

The area covered by PLP was measured in the three subregions of mPFC (prelimbic, infralimbic and cingulate), as well as in barrel cortex of PND90 APO-SUS and APO-UNSUS male rats. The analysis showed that PLP coverage was significantly lower in the prelimbic and infralimbic cortices of APO-SUS. In cingulate and barrel cortices, no significant differences between the two groups were observed.

4. Discussion

4.1. Redox imbalance occurs early in life of APO-SUS rats

Molecular analysis of redox-related gene expression demonstrated that signs of lower redox capacity are already present at the age of PND21 throughout the brains of the APO-SUS rats. This finding is in agreement with the results of previous studies in older APO-SUS and APO-UNSUS rats as well as with the association of schizophrenia with oxidative stress in human patients (Flatow et al., 2013; Monin et al., 2014). The fact that Gstm4 was not differentially expressed in the mPFC and CC of the PND21 rats is in line with previous observations (Maas, D., de Kleijn, K., unpublished data) and could be attributed to the large inter-individual variation in the expression of this gene that has also been detected in humans (Kearns et al., 2003).

This observed dysregulation of two redox-related enzymes is, however, only a mere indication of redox imbalance. To confirm the presence of such a disturbance in the APO-SUS rats, a more direct assessment of redox and oxidative stress is required. One way to achieve this is by measuring mitochondrial ROS production directly (Starkov, 2010). Another approach is to measure biomarkers of oxidative stress, namely byproducts of oxidative damage on biomolecules. For this purpose, we could assess a) ROS-induced DNA damage through immunostaining for 8-oxo-2'-deoxyguanosine (8-oxo-dG), the oxidized derivative of deoxyguanosine (Machella et al., 2004), b) protein carbonylation through ELISA or Western blot immunoassay (Dalle-Donne et al., 2003) and c) lipid peroxidation from the levels of thiobarbituric acid-reactive substances (TBARS) (Falone et al., 2012) or F2-isoprostanes (Milatovic & Aschner, 2009). Alternatively, we could quantify antioxidant activity in the brain regions of interest (Shea et al., 2003). For an overview of oxidative stress tests, see the reviews by Palmieri & Sblendorio (2007) and Ho et al. (2013).

Furthermore, whether redox imbalance affects (neuro)development has not yet been established. Examination of APO-SUS rats younger than PND21 would show whether antioxidant defense in the brains of these animals is compromised since birth. This knowledge would aid us in the search of a potential treatment approach for SZ's myelination disturbances that are thought to be caused by oxidative stress. Such an approach could involve direct manipulation of redox through administration of antioxidants. If this application is proven capable to rescue myelination deficits in mPFC of APO-SUS, it would strengthen the hypothesised link between redox imbalance and demyelination in SZ and

provide a promising potential mechanism for the prevention of schizophrenia-related cognitive decline. In a relevant study, Cabungcal et al. (2014) have found that treating juvenile and adolescent rats of a developmental model for SZ with the antioxidant N-acetyl cysteine or with the glutathione peroxidase mimic ebselen can prevent the model's characteristic SZ-related deficits that are observed in adults.

4.2 Myelin- and OL-related abnormalities in APO-SUS rats occur progressively

While differential expression of redox-related genes in the mPFC was consistent among different ages, myelin-related gene hypoexpression was significantly less prominent in PND21 APO-SUS than in PND28 and older rats. This finding supports the hypothesis that the hypomyelination of mPFC has a progressive nature, similar to the trajectory of SZ's cognitive symptoms and the results of cellular analysis are also in agreement. In line with these results, studies in schizophrenic patients have observed progressive abnormalities in both gray and white matter, pointing towards an age-related component in the development of the disorder (van Haren et al., 2007; Olabi et al., 2011; Vita et al., 2012). Likewise, although at the mRNA level OL-related gene expression was similar for the two lines in any of the ages tested, cell density measurement uncovered a clear decrease in OLs in the mPFC of young-adult PND90 APO-SUS males. At PND21 this difference was not yet established and the two lines had comparable OL numbers, suggesting that OL density starts to decline at a developmental stage between PND21 and PND90. Similarly, Vostrikov and Uranova (2011) found that OLs in gray and white matter of patients with SZ did not follow the age-related increase in number that is observed in healthy individuals. Also, Bartzokis et al. (as reviewed in Bartzokis et al., 2012) have proposed that the normal myelination trajectory is dysregulated in SZ patients. Hence, there seems to be a disturbance in the maturational processes of myelination in SZ.

Taken together, our analysis in mPFC leads to the assumption that redox-related gene dysregulation in APO-SUS rats precedes the emergence of extensive disturbances in myelination, which seem to be age related.

4.3 Myelination deficits in APO-SUS rats display region specificity

4.3.1 mPFC

The observed abnormalities related to myelin and OLs appear predominantly in the mPFC of APO-SUS rats, both at a molecular and a cellular level. More specifically, myelin-related genes are significantly hypoexpressed in the prelimbic and infralimbic subregions of mPFC, but no such differences were present in corpus callosum or striatum. Furthermore, while, as previously seen in older ages (Maas, D. et al., unpublished results), characterization at mRNA level did not reveal effects on OL-related gene expression, cellular analysis revealed that OL density is affected in all three mPFC subregions. Corpus callosum, that was again used as control, did not demonstrate any differences between APO-UNSUS and APO-SUS and the results for striatum were inconclusive, as discussed in the next section. mPFC specificity is also supported by the IHC analysis of the myelin proteolipid protein (PLP).

Quantification of the major CNS myelin protein showed that APO-SUS had lower density of myelinated axons only in subregions of their mPFC (prelimbic and infralimbic) and not in the cortical region we used as a control, namely the barrel cortex. The region specificity of these myelination impairments in the PFC of APO-SUS rats is analogous to the alterations in the prefrontal circuitry of SZ patients that have been proposed to underlie cognitive deficits (Sakurai et al., 2015). To take our investigation a step further, we could perform immunohistochemistry targeting neurofilament and look for potential aberrations in axonal integrity. Axonal integrity has been demonstrated to be altered in gray and white matter of the PFC in SZ, presumably due to the insufficient oligodendroglial support that causes axonal atrophy (Uranova et al., 2011). Also, it would be of interest to extend the analysis of PLP quantification to other ages, especially prior to PND90 and to include markers of other myelin-related proteins like MBP, in order to shed light on the developmental trajectory myelination in SZ.

Another observation that distinguishes the PFC from other brain regions in terms of myelination is the OPC-to-OL ratio, which was higher in mPFC (especially prelimbic and infralimbic) than in other brain regions of both rat lines for both the tested ages. Hence, there are more OPCs in relation to the OL density in the mPFC than in corpus callosum, striatum or hippocampus, which could be associated to the later maturation of myelination in this cortical region (Fuster, 2002).

Moreover, the cingulate cortex is a region that should be further investigated in order to shed light on the link between its myelination and the occurrence of schizophrenia. In primates, the anterior cingulate cortex (ACC) integrates sensory and emotional input from multiple brain areas and is involved in multiple functions, including the regulation of cognitive control (Jones and Powell, 1970; Carter and van Veen, 2007). Although previous research has repeatedly associated SZ with aberrations in this area (Fornito et al., 2009; Höistad et al., 2009; Cui et al., 2015), our study found myelination deficits in the cingulate of APO-SUS only in terms of OL density and not at gene expression or PLP quantification.

4.3.2 Corpus callosum and striatum

Corpus callosum of APO-SUS did not show any myelination deficits in general. An exception was observed in one out of the seven tested genes per age group, but the statistical significance of this result should be further inspected through multiple testing corrections.

Regarding the striatum, although mRNA expression analysis did not reveal myelination deficits, OL quantification showed some alterations between APO-SUS and APO-UNSUS. On the one hand, the decreased OL density in the dorsolateral striatum of PND90 APO-SUS is in agreement with recent indications of myelination disturbances in the dorsolateral striatum of female APO-SUS (de Kleijn, K., unpublished data). On the other hand, the detected decrease in OLs in the dorsomedial striatum of APO-SUS was unexpected, especially since it was observed in the younger group (PND21) only. A possible explanation could be that the size or the location of the counting frame weren't optimal, as striatum is a brain area whose subregions do not always have clear boundaries (Suppl. Fig. 1). In any case,

the separate examination of dorsolateral and dorsomedial striatum seems to be critical due to their distinctive structure and function (Rodriguez et al., 2006; Corbit & Janak, 2007). Furthermore, although in the present study striatum is used as a control region for comparisons with the late-maturing PFC at the level of myelination, there are suggestions for its contribution to the development of cognitive symptoms in SZ through the striatal-cortical circuitry (Simpson et al., 2010; Beasley et al., 2009; Chuhma et al., 2016).

4.3.3 Hippocampus (CA4)

The hippocampus is an extensively studied area and multiple studies have linked anatomical and functional alterations of this formation with schizophrenia (Chambers et al., 2001; Tamminga et al., 2010; Ledoux et al., 2013). However, other researchers like Walker and her colleagues (2002) have found that the volume and cellular composition of the hippocampus and its subfields did not differ between SZ patients and healthy control subjects. We investigated the cell density of OLs and OPCs in the hilus (CA4 subregion) and observed decreased OPC density in PND21 APO-SUS and decreased OL density in PND90, suggesting that OPC survival is afflicted in pre-adolescent ages and that this would result in decreased numbers of mature OLs in adult brains. A recent study (Falkai et al., 2016) demonstrated that SZ patients with cognitive dysfunction have a decreased number of OLs in CA4 of the anterior and not the posterior hippocampus, so it would be interesting to search for such differences in the APO-SUS/APO-UNSUS model, as well as to look into the other subregions of the hippocampal formation.

4.4 OPC maturation and proliferation in the APO-SUS mPFC

One of our research questions was whether the potential OL deficits can be attributed to either OPC differentiation or proliferation. The cell density assessment in mPFC showed that only mature OLs are decreased in APO-SUS at PND90, while at PND21 OLs are not yet affected, similarly to OPCs in two out of the three subregions. Taking into account the OPC/OL ratio, it is clear that significantly less OPCs have managed to differentiate to mature OLs, proposing that OL decrease is probably caused by impairments in OPC maturation in the mPFC and not proliferation. This interpretation is in line with findings in post-mortem mPFC of SZ patients that pointed towards an impaired OPC differentiation in SZ (Mauney et al., 2015). Additionally, as mentioned earlier, one of the threats against the formation of mature OLs is oxidative stress (French et al., 2009; Monin et al., 2014), which, according to our findings, seems to be present in the PFC of APO-SUS rats early in development. These observations suggest a mechanism that associates myelination deficits in SZ with oxidative stress, through an apparent failure in OPC differentiation.

A future application of IHC with the use of other markers specific for the various stages of OL differentiation and maturation, such as the antibody CC-1 (anti-APC, detects the protein adenomatous polyposis coli) for mature myelinating OLs and the proliferation marker bromodeoxyuridine (BrdU) would help us reach a safer conclusion on this matter. Also, in

order to get insight into the cellular morphology of OPCs and OLs as well as on the thickness of myelin, electron microscopy would be the method of choice.

4.5 Conclusion

In conclusion, the findings of the present study strengthen the hypothesis for a connection in schizophrenia between presymptomatic oxidative stress and localized myelination deficits in the late-maturing PFC. Furthermore, these myelination abnormalities seem to have an age-related component that is concomitant to the onset of the disorder. Altogether, our study contributes to a better understanding of the mechanisms underlying myelination deficits in SZ and aims to assist the efforts towards the development of pharmacological strategies to treat or even prevent the associated cognitive symptoms.

Acknowledgements

First of all, I would like to express my sincere gratitude to dr. Astrid Vallès Sanchez for being an inspiring on-site supervisor, and a patient and supportive advisor throughout my internship. Also, I would like to thank my educational supervisor, prof. dr. Gerard Martens, for giving me the opportunity to take part in a project I was so much interested in and for our stimulating discussions on my work. Finally, I would like to express my gratitude to the other members of the Molecular Animal Physiology Department for always being helpful and for creating such a pleasant workplace. This internship was a great learning experience for me and it broadened my perspective of science.

References

American Psychiatric Association (1994) Diagnostic and Statistical Manual of Mental Disorders — (DSM-IV), 4th edition. American Psychiatric Association, Washington D.C.

Andersen, S. L. (2003) Trajectories of brain development: point of vulnerability or window of opportunity? Neurosci Biobehav Rev. 2003; 27:3–18.

Amaral, D. G. (1978). A Golgi Study of Cell Types in the Hilar Region of the Hippocampus in the Rat, 851–914.

Barch, D. M., Bustillo, J., Gaebel, W., Gur, R., Heckers, S., Malaspina, D., … Carpenter, W. (2013). Logic and justification for dimensional assessment of symptoms and related clinical phenomena in psychosis: Relevance to DSM-5. Schizophrenia Research. http://doi.org/10.1016/j.schres.2013.04.027

Bartzokis, G., Lu, P. H., Raven, E. P., Amar, C. P., Detore, N. R., Couvrette, A. J., ... & Subotnik, K. L. (2012). Impact on intracortical myelination trajectory of long acting injection

versus oral risperidone in first-episode schizophrenia. Schizophrenia research, 140(1), 122-128.

Beasley, C. L., Dwork, A. J., Rosoklija, G. et al. (2009). Metabolic abnormalities in fronto-striatal-thalamic white matter tracts in schizophrenia. Schizophrenia Research, vol. 109, no. 1–3, pp. 159–166.

Bitanihirwe, B. K., Woo, T.-U.W. (2011). Oxidative stress in schizophrenia: an integrated approach. Neurosci Biobehav Rev. 35:878–893.

Bora, E., Yucel, M., & Pantelis, C. (2009). Cognitive functioning in schizophrenia, schizoaffective disorder and affective psychoses : meta-analytic study, 475–482. http://doi.org/10.1192/bjp.bp.108.055731

Butts, B. D., Houde, C., & Mehmet, H. (2008). Maturation-dependent sensitivity of oligodendrocyte lineage cells to apoptosis: implications for normal development and disease. Cell Death and Differentiation, 15(7), 1178–1186. http://doi.org/10.1038/cdd.2008.70

Cabungcal, J. H., Counotte, D. S., Lewis, E. M., Tejeda, H. A., Piantadosi, P., Pollock, C., … O'Donnell, P. (2014). Juvenile Antioxidant Treatment Prevents Adult Deficits in a Developmental Model of Schizophrenia. Neuron, 83(5), 1073–1084. http://doi.org/10.1016/j.neuron.2014.07.028

Callicott, J. H., Mattay, V. S., Verchinski, B. A., Marenco, S., Egan, M. F., and Weinberger, D. R. (2003). Complexity of prefrontal cortical dysfunction in schizophrenia: more than up or down. Am. J. Psychiatry 160, 2209–2215.

Carter, C. S., and van Veen, V. (2007). Anterior cingulate cortex and conflict detection: an update of theory and data. Cogn. Affect. Behav. Neurosci. 7, 367–379. doi: 10.3758/CABN.7.4.367

Catts, V. S., Fung, S. J., Long, L. E., Joshi, D., Vercammen, A., Allen, K. M., … Weickert, C. S. (2013). Rethinking schizophrenia in the context of normal neurodevelopment, 7(May), 1–27. http://doi.org/10.3389/fncel.2013.00060

Chambers, R. A., Krystal, J. H., & Self, D. W. (2001). Neurobiological Basis for Substance Abuse Comorbidity in Schizophrenia. Biol Psychiatry 75; 50:71– 83

Chen, Q., Chen, X., He, X., Wang, L., Wang, K., & Qiu, B. (2016). Neuroscience Letters Aberrant structural and functional connectivity in the salience network and central executive network circuit in schizophrenia. Neuroscience Letters, 627, 178–184. http://doi.org/10.1016/j.neulet.2016.05.035

Chuhma, N., Mingote, S., Kalmbach, A., Yetnikoff, L., & Rayport, S. (2016). Heterogeneity in Dopamine Neuron Synaptic Actions Across the Striatum and Its Relevance for Schizophrenia. Biological Psychiatry, 1–9. http://doi.org/10.1016/j.biopsych.2016.07.002

Corbit, L. H., & Janak, P. H. (2007). Inactivation of the Lateral But Not Medial Dorsal Striatum Eliminates the Excitatory Impact of Pavlovian Stimuli on Instrumental Responding, 27(51), 13977–13981. http://doi.org/10.1523/JNEUROSCI.4097-07.2007

Cui, L., Liu, J., Wang, L., Li, C., Xi, Y., & Guo, F. (2015). Anterior cingulate cortex-related connectivity in first-episode schizophrenia: a spectral dynamic causal modeling study with functional magnetic resonance imaging, 9(November), 1–10. http://doi.org/10.3389/fnhum.2015.00589

Dalle-Donne, I., Rossi, R., Giustarini, D., Milzani, A., & Colombo, R. (2003). Protein carbonyl groups as biomarkers of oxidative stress. Clinica Chimica Acta 329 (2003) 23–38. http://doi.org/10.1016/S0009-8981(03)00003-2

Davis K. L., Stewart D. G., Friedman J.I., et al. (2003). White Matter Changes in Schizophrenia: Evidence for Myelin-Related Dysfunction. Arch Gen Psychiatry. 60(5):443-456. doi:10.1001/archpsyc.60.5.443.

Davis, K. L., Stewart, D. G., Friedman, J. I., & Buchsbaum, M. (2013). White Matter Changes in Schizophrenia, 60(May 2003), 443–456.

Do, K. Q., Cabungcal, J. H., Frank, A., Steullet, P., Cuenod, M. (2009) Redox dysregulation, neurodevelopment, and schizophrenia. Curr Opin Neurobiol. 19:220–230.

Ellenbroek, B. A., & Cools, A. R. (2000). Animal models for the negative symptoms of schizophrenia. Behav Pharmacol, 11(3-4), 223-233.

Ellenbroek, B. A., & Cools, A. R. (2002). Apomorphine susceptibility and animal models for psychopathology: Genes and environment. Behavior Genetics, 32(5), 349–361. http://doi.org/10.1023/A:1020214322065

Ellenbroek, B. A., Geyer, M. A., & Cools, A. R. (1995). The behavior of APO-SUS rats in animal models with construct validity for schizophrenia. J Neurosci, 15(11), 7604-7611.

van der Elst, M.C.J., Verheij, M.M.M., Roubos, E.W., Ellenbroek, B.A., Veening, J.G., Cools, A.R. (2005). A single exposure to novelty differentially affects the accumbal

dopaminergic system of apomorphine-susceptible and apomorphine-unsusceptible rats. Life Sciences, 76: 1391-1406.

Emery, B. (2010). Regulation of oligodendrocyte differentiation and myelination. Science, 330(6005):779-82. doi: 10.1126/science.1190927.

Eslinger, P.J., Flaherty-Craig, C.V., Benton, A.L. (2004) Developmental outcomes after early prefrontal cortex damage. Brain Cogn. 55, 84 – 103.

Falone, S., Alessandro, A. D., Mirabilio, A., Cacchio, M., Ilio, C. Di, Loreto, S. Di, & Amicarelli, F. (2012). Late-Onset Running Biphasically Improves Redox Balance, Energy- and Methylglyoxal-Related Status, as well as SIRT1 Expression in Mouse Hippocampus. PLoS One. 2012;7(10): e48334. doi: 10.1371/journal.pone.0048334

Fisher, A. B. (2011). Peroxiredoxin 6: a bifunctional enzyme with glutathione peroxidase and phospholipase A_2 activities. Antioxid Redox Signal, 15(3):831-44. doi: 10.1089/ars.2010.3412. Epub 2011 Mar 31.

Flatow, J., Buckley, P., and Miller, B.J. (2013). Meta-analysis of oxidative stress in schizophrenia. Biol. Psychiatry 74, 400–409.

Flynn, S.W., Lang, D.J., Mackay, A.L., Goghari, V., Vavasour, I.M., Whittall, K.P., Smith, G.N., Arango, V., Mann, J.J., Dwork, A.J., Falkai, P., Honer, W.G. (2003). Abnormalities of myelination in schizophrenia detected in vivo with MRI, and post-mortem with analysis of oligodendrocyte proteins. Mol. Psychiatry 8 (9), 811–820.

Fornito, A., Yu, M., Dean, B., Wood, S., Pantelis, C. (2009). Anatomical Abnormalities of the Anterior Cingulate Cortex in Schizophrenia: Bridging the Gap Between Neuroimaging and Neuropathology. Schizophrenia Bulletin vol. 35 no. 5 pp. 973–993, 2009 doi:10.1093/schbul/sbn025

French, H. M., Reid, M., Mamontov, P., Simmons, R. A., & Grinspan, J. B. (2009). Oxidative stress disrupts oligodendrocyte maturation. Journal of Neuroscience Research, 87(14), 3076–3087. http://doi.org/10.1002/jnr.22139

Fuster,, J. M. (2002). Frontal lobe and cognitive development. J. Neurocytol. 31, 373–385.

Goldberg, T. E., & Green, M. F. (1995). NEUROCOGNITIVE FUNCTIONING IN PATIENTS WITH SCHIZOPHRENIA: AN OVERVIEW.

Goldman-Rakic, P. S, Selemon, L. D. (1997) Functional and anatomical aspects of prefrontal pathology in schizophrenia. Schizophr Bull. 23:437- 121. 458

Hakak, Y., Walker, J. R., Li, C. et al. (2001) Genome-wide expression analysis reveals dysregulation of myelination-related genes in chronic schizophrenia. Proc. Natl Acad. Sci. USA 98: 4746–51.

van Haren, N. E. M., Cahn, W., Pol, H. E. H., & Kahn, R. S. (2008). Schizophrenia as a progressive brain disease. European Psychiatry 23, 245-254. http://doi.org/10.1016/j.eurpsy.2007.10.013

Haroutunian, V., Katsel, P., Roussos, P., Davis, K. L., Altshuler, L. L., & Bartzokis, G. (2014). Myelination, oligodendrocytes, and serious mental illness. Glia, 62(11), 1856–1877. http://doi.org/10.1002/glia.22716

Ho, E., Karimi, K., Liu, C., Bhindi, R., & Figtree, G. A. (2013). Biological markers of oxidative stress: Applications to cardiovascular research and practice. Redox Biology, 1(1), 483–491. http://doi.org/10.1016/j.redox.2013.07.006

Höistad, M., Segal, D., Takahashi, N., Sakurai, T., Buxbaum, J. D., & Hof, P. R. (2009). Linking white and grey matter in schizophrenia: oligodendrocyte and neuron pathology in the prefrontal cortex. Front Neuroanat., 3(July), 1–16. http://doi.org/10.3389/neuro.05.009.2009

Jones, E. G., & Powell, T. P. (1970). An anatomical study of converging sensory pathways within the cerebral cortex of the monkey. Brain 93, 793–820.

Kearns, P. R., Chrzanowska-lightowlers, Z. M. A., Pieters, R., & Veerman, A. (2003). Mu class glutathione S-transferase mRNA isoform expression in acute lymphoblastic leukaemia. British Journal of Haematology, 120, 80–88.

Ledoux, A.A., Phillips, J.L., Labelle, A., Smith, A., Bohbotc, V.D., & Boyer, P. (2013). Decreased fMRI activity in the hippocampus of patients with schizophrenia compared to healthy control participants, tested on a wayfinding task in a virtual town, Psychiatry Research: Neuroimaging 211, 47–56. http://doi.org/10.1016/j.pscychresns.2012.10.005

Lewandowski, K. E., Cohen, B. M., Keshavan, M. S., & Öngür, D. (2011). Relationship of Neurocognitive Deficits to Diagnosis and Symptoms across Affective and Non-Affective Psychoses. Schizophrenia Research, 133(1-3), 212–217. http://doi.org/10.1016/j.schres.2011.09.004

Lewis, D. A. (1997) Development of the prefrontal cortex during adolescence: insights into vulnerable neural circuits in schizophrenia. Neuropsychopharmacology. 16:385–398.

Machella, N., Regoli, F., Cambria, A., & Santella, R. M. (2004). Oxidative damage to DNA: an immunohistochemical approach for detection of 7, 8-dihydro-8-oxodeoxyguanosine in marine organisms. Marine Environmental Research 58 (2004) 725–729. http://doi.org/10.1016/j.marenvres.2004.03.022

Mauney, S. A., Pietersen, C. Y., Sonntag, K., & Woo, T. W. (2015). Differentiation of oligodendrocyte precursors is impaired in the prefrontal cortex in schizophrenia. Schizophrenia Research, 169(1-3), 374–380. http://doi.org/10.1016/j.schres.2015.10.042

Milatovic, D. and Aschner, M. (2009). Measurement of Isoprostanes as Markers of Oxidative Stress in Neuronal Tissue. Curr Protoc Toxicol. 2009(Supplement 39): 12.14.1–12.14.12. doi: 10.1002/0471140856.tx1214s39.

Miller, E. K., Freedman, D. J., & Wallis, J. D. (2002). The prefrontal cortex: categories, concepts and cognition, (July), 1123–1136. http://doi.org/10.1098/rstb.2002.1099

Minzenberg, M. J., Lesh, T. A., Niendam, T. A., Yoon, J. H., Rhoades, R. N., & Carter, C. S. (2014). Frontal cortex control dysfunction related to long-term suicide risk in recent-onset schizophrenia. Schizophr Res, 157(1-3), 19-25. doi: 10.1016/j.schres.2014.05.039

Monin, A., Baumann, P. S., Griffa, a, Xin, L., Mekle, R., Fournier, M., … Do, K. Q. (2014). Glutathione deficit impairs myelin maturation: relevance for white matter integrity in schizophrenia patients. Molecular Psychiatry, (April), 1–12. http://doi.org/10.1038/mp.2014.88

Nave, K.A. and Werner, H.B. (2014). Myelination of the nervous system: mechanisms and functions. Annu. Rev. Cell Dev. Biol. 30, 503–533

Olabi B, Ellison-Wright I, McIntosh AM, Wood SJ, Bullmore E, Lawrie SM. (2011). Are there progressive brain changes in schizophrenia? A meta- analysis of structural magnetic resonance imaging studies. Biol Psychiatry 70: 88–96.

Palmieri, B. and Sblendorio, V. (2007). Oxidative stress tests: overview on reliability and use Part I, European Review for Medical and Pharmacological Sciences, 309–342.

Pastore, A., Federici, G., Bertini, E., & Piemonte, F. (2003). Analysis of glutathione: implication in redox and detoxification, 333, 19–39. http://doi.org/10.1016/S0009-8981(03)00200-6

Potkin, S. G., Turner, J. A., Brown, G. G., McCarthy, G., Greve, D. N., Glover, G. H., et al. (2009). Working memory and DLPFC inefficiency in schizophrenia: the FBIRN study. Schizophr. Bull. 35, 19–31.

Reddy, R. D., Yao, J. K. (1996). Free radical pathology in schizophrenia: a review. Prostaglandins Leukot Essent Fatty Acids. 55:33–43.

Reichenberg, A., Harvey, P. D., Bowie, R., Mojtabai, R., Rabinowitz, J., Heaton, R. K., & Bromet, E. (2009). Neuropsychological Function and Dysfunction in Schizophrenia and Psychotic Affective Disorders, 35(5), 1022–1029. http://doi.org/10.1093/schbul/sbn044

Rodriguez, M., Morales, I., Gomez, I., Gonzalez, S., Gonzalez-hernandez, T., & Gonzalez-mora, J. L. (2006). Heterogeneous Dopamine Neurochemistry in the Striatum: The Fountain-Drain Matrix. J Pharmacol Exp Ther. 2006 Oct; 319(1), 31–43. http://doi.org/10.1124/jpet.106.104687

Sakurai, T., Gamo, N. J., Hikida, T., Kim, S., Murai, T., Tomoda, T., & Sawa, A. (2015). Progress in Neurobiology Converging models of schizophrenia – Network alterations of prefrontal cortex underlying cognitive impairments. Progress in Neurobiology, 134, 178–201. http://doi.org/10.1016/j.pneurobio.2015.09.010

Schneider, M., & Koch, M. (2005). Behavioral and morphological alterations following neonatal excitotoxic lesions of the medial prefrontal cortex in rats. Experimental Neurology, 195(1), 185–198. http://doi.org/10.1016/j.expneurol.2005.04.014

Shea, T. B., Rogers, E., Ortiz, D., & Sheu, M. (2003). Quantification of antioxidant activity in brain tissue homogenates using the " total equivalent antioxidant capacity" Journal of Neuroscience Methods 125, 55–58. http://doi.org/10.1016/S0165-0270(03)00028-1

Simpson, E. H., Kellendonk, C., & Kandel, E. (2010). Perspective A Possible Role for the Striatum in the Pathogenesis of the Cognitive Symptoms of Schizophrenia. Neuron, 65(5), 585–596. http://doi.org/10.1016/j.neuron.2010.02.014

Starkov, A. (2010). Measurement of Mitochondrial ROS Production. Methods Mol Biol. 2010; 648: 245–255. doi:10.1007/978-1-60761-756-3_16.

Tamminga C.A., Stan, A. D., & Wagner, A. D. (2010). The Hippocampal Formation in Schizophrenia. Am J Psychiatry 2010; 167:1178–1193.

Tan, H. Y., Sust, S., Buckholtz, J. W., Mattay, V. S., Meyer-Lindenberg, A., Egan, M. F., et al. (2006). Dysfunctional prefrontal regional specialization and compensation in schizophrenia. Am. J. Psychiatry 163, 1969–1977.

Tandon, R., Gaebel, W., Barch, D. M., Bustillo, J., Gur, R. E., Heckers, S., … Carpenter, W. (2013). De fi nition and description of schizophrenia in the DSM-5. http://doi.org/10.1016/j.schres.2013.05.028

Tomassy, G. S., Dershowitz, L. B., & Arlotta, P. (2015). Diversity Matters: A Revised Guide to Myelination. Trends in Cell Biology, xx, 1–13. http://doi.org/10.1016/j.tcb.2015.09.002

Uranova, N.A., Vikhreva, O.V., Rachmanova, V.I., Orlovskaya, D.D. (2011). Ultrastructural alterations of myelinated fibers and oligodendrocytes in the prefrontal cortex in schizophrenia: a postmortem morphometric study. Schizophr. Res. Treat. 2011, 325789.

National Institute of Mental Health, National Institutes of Health, U. S. Department of Health and Human Services, (2015). Schizophrenia (NIH Publication No. 15-3517). Retrieved from http://www.nimh.nih.gov/health/publications/schizophrenia-booklet-12-2015/index.shtml

Vandesompele, J., De Preter, K., Pattyn, F., Poppe, B., Van Roy, N., De Paepe, A., Speleman, F. (2002). Accurate normalization of real-time quantitative RT-PCR data by geometric averaging of multiple internal control genes. Genome Biology, 3, 34.1-34.11.

Vartanian, T., Fischbach, G., Miller, R. (1999). Failure of spinal cord oligodendrocyte development in mice lacking neuregulin. Proc Natl Acad Sci U S A. 96:731-735.

Vikhreva, O.V., Rakhmanova V.I., Orlovskaya D.D., Uranova N.A. (2016). Ultrastructural alterations of oligodendrocytes in prefrontal white matter in schizophrenia: A post-mortem morphometric study. Schizophr Res, pii: S0920-9964(16)30173-6. doi: 10.1016/j.schres.2016.04.023.

Vita A., De Peri L., Deste G., Sacchetti E. (2012). Progressive loss of cortical gray matter in schizophrenia: A meta-analysis and meta-regression of longitudinal MRI studies. Transl Psychiatry 2; e190.

Vostrikov, V., Uranova, N. (2011). Age-related increase in the number of oligodendrocytes is dysregulated in schizophrenia and mood disorders. Schizophr. Res. Treat. 2011, 174689.

Walker, M. A., Highley, J. R., Phil, D., Mcdonald, B., Path, M. R. C., Roberts, H. C., … Psych, F. R. C. (2002). Estimated Neuronal Populations and Volumes of the Hippocampus and Its Subfields in Schizophrenia. Am J Psychiatry 2002; 159:821–828.

Woo, T.-U. W. (2014). Neurobiology of Schizophrenia Onset. Current Topics in Behavioral Neurosciences, 16, 267–295. http://doi.org/10.1007/7854_2013_243

Yao, J. K., Reddy, R. D., van Kammen, D. P. (2001). Oxidative damage and schizophrenia: an overview of the evidence and its therapeutic implications. CNS Drugs. 15:287–310.

Supplementary Material

Supplemental Table 1. Primer sequences for RNA expression analysis

Gene category	Gene	Forward primers 5'-3'	Forward primers 5'-3'
Housekeeping	β-Actin	CCTTCCTGGGTATGGAATCCTGT	TAGAGCCACCAATCCACACA
	Cyc-A	AGCACTGGGGAGAAAGGATT	AGCCACTCAGTCTTGGCAGT
	Gapdh	GGGTGTGAACCACGAGAAAT	ACTGTGGTCATGAGCCCTTC
	Ywhaz	TTGAGCAGAAGACGGAAGGT	GAAGCATTGGGGATCAAGAA
Redox-related	Prdx6	TGACTGGAAGAAGGGAGAGAGTGT	ATGGGAGCTCTTTGGTGAAGAC
	Gstm4	GCCTAGGCCCCTGGTTTTC	TCTTCACAGCAGCACAGCAACT
Myelin-related	Mbp	CCCTACTCCATCCTCAGACTTTCTT	TGGCGGTGTGCCTGTCTAT
	Plp1	GGGCCTGAGCGCAACGGTAA	CAGGCACAGCAGAGCAGGCAA
	Mag	AAGCCAGACCATCCAACCTTC	CTCCTGATTCCGCTCCAAGT
	Mog	CGCCGTGGAGTTGAAAGTAG	GCACGGAGTTTTCCTCTAGT
	Mobp	AATACCTGCAGGGCAACAAAG	TCTGGTTCTTGGAGAGCCTGG
	Cldn11	CGCAAAATGGACGAACTGGG	TGCACGTAACCAGGGAGGAT
	Opalin	ACCCTGATCCAGCGAAGAAG	TGACTGCCTAGGATTCTCGGATA
OL transcription factors	Sox10	GCTCTGGAGGTTGCTGAACGA	GTAGTGAGCCTGGATAGCAGC
	Olig2	GCTTCACAGGAGGAACCGTG	TTCTTGGTGGAAGACGTGGC
OPC	PdgfαR	ATGCGTGTGGACTCTGACAA	CTGCGAGCTGTGTCTGTTCC
Astrocyte marker	Gfap	AAAACCGCATCACCATTCCTG	CTCCACCGTCTTTACCACGA

Supplemental Figure 1. Tissue collection for mRNA isolation
A. mPFC punch **B**. Whole dorsal striatum punches **C**. Corpus callosum microdissection

Supplemental Table 2. Antibodies used in IHC

Epitope	Primary antibody	Specificity	Secondary antibody
OLIG2	Anti-OLIG2 rabbit monoclonal [EPR2673], ab109186, Abcam	Whole OL lineage	Alexa fluor 555 goat-anti-rabbit, Jackson Immuno Research
NG2 Chondroitin Sulfate Proteoglycan	Anti-NG2 mouse monoclonal, MAB5384, Millipore	OPCs and blood vessels	Alexa fluor 488 goat-anti-mouse, Jackson Immuno Research
PLP	Anti-PLP mouse monoclonal, clone plpc1, MCA839G, Bio-Rad	Myelin sheath	Alexa fluor 488 goat-anti-mouse, Jackson Immuno Research

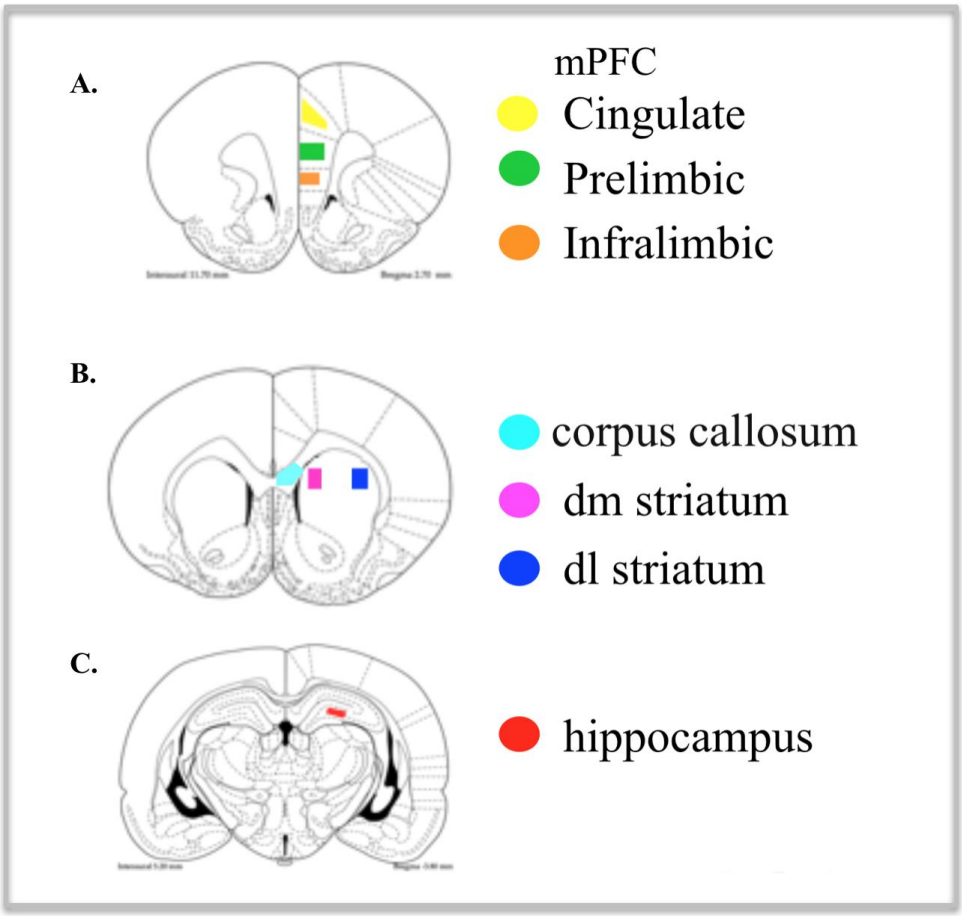

Supplemental Figure 2. Regions of interest for IHC

Analysed areas in: **A**. mPFC. Cingulate cortex is coloured here yellow, prelimbic cortex is green and infralimbic is the orange bin. **B**. Corpus callosum and striatum. Light blue indicates the bin of corpus callosum, while magenda shows the measured area of the medial striatum and dark blue of the lateral striatum. **C**. Hippocampus. The analysed area was CA4 (red), a CA part enclosed by the dentate gyrus (images adjusted from Paxinos and Watson, 1998).

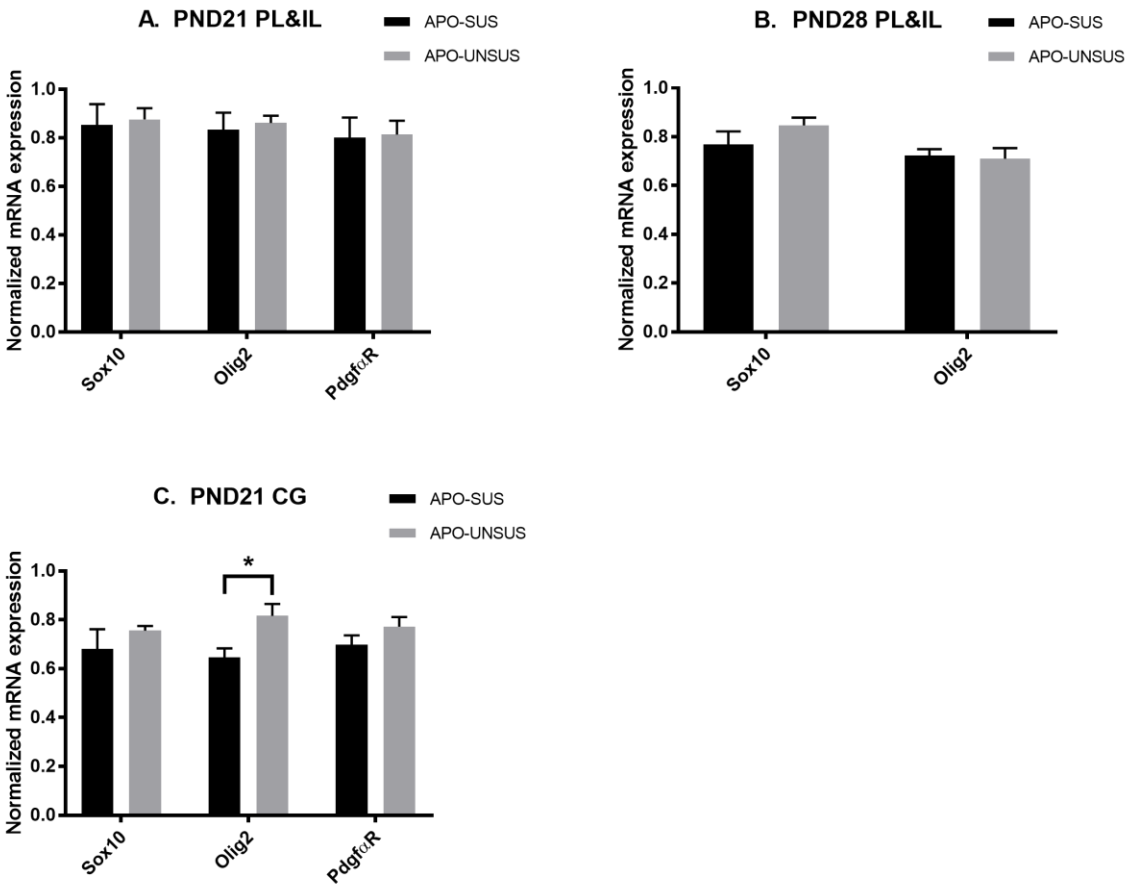

Supplemental Figure 3. mRNA expression of OL-related genes in the mPFC of PND21 and PND28 APO-SUS and APO-UNSUS rats

The bars represent the mean normalised mRNA expression of Sox10, Olig2 and PdgfaR in APO-SUS (black) and APO-UNSUS (grey), along with error bars for the standard error of the mean. The asterisk (*) indicates statistically significant difference ($p \leq 0.05$) in gene expression between APO-SUS and APO-UNSUS, which was determined by the independent samples Student's t-test after removal of the outliers by the Grubbs test for outliers. **A**. Normalised OL-related gene expression in prelimbic and infralimbic cortices of PND21 APO-SUS and APO-UNSUS rats (n=7-8 per group). Samples were normalized against the housekeeping genes β-Actin and Cyc-A. **B**. Normalised OL-related gene expression in prelimbic and infralimbic cortices (PL&IL) of PND28 APO-SUS and APO-UNSUS rats (n=7-8 per group). Samples were normalized against the housekeeping genes Gapdh and Ywhaz. **C**. Normalised OL-related gene expression in cingulate cortex of PND21 APO-SUS and APO-UNSUS rats (n=5-8 per group). Samples were normalized against the housekeeping genes β-actin and Ywhaz.

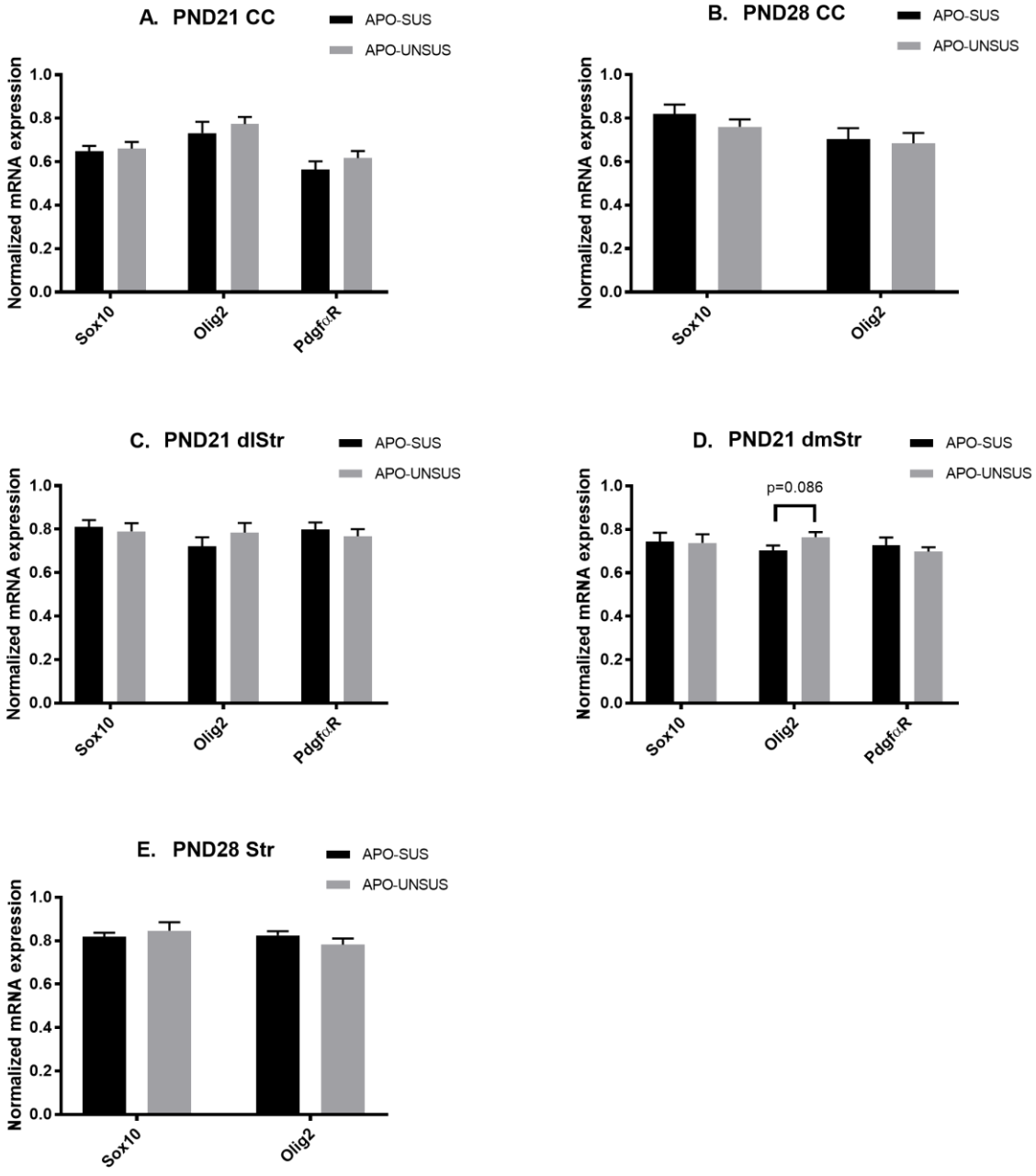

Supplemental Figure 4. mRNA expression of OL-related genes in corpus callosum and striatum of PND21 and PND28 APO-SUS and APO-UNSUS rats

The bars represent the mean normalised mRNA expression of Sox10, Olig2 and PdgfaR in APO-SUS (black) and APO-UNSUS (grey), along with error bars for the standard error of the mean. Statistical significance in gene expression between APO-SUS and APO-UNSUS was determined by the independent samples Student's t-test ($p \leq 0.05$) after removal of the outliers by the Grubbs test for outliers. **A**. Mean normalised mRNA expression in corpus callosum of PND21 APO-SUS and APO-UNSUS rats (n=7-8 per group). Samples were normalized against the housekeeping genes β-Actin and Cyc-A. **B**. Mean normalised mRNA expression in corpus callosum of PND28 APO-SUS and

APO-UNSUS rats (n=8 per group). Samples were normalized against the housekeeping genes Cyc-A and Ywhaz. **C**. Mean normalised mRNA expression in dorsolateral striatum of PND21 APO-SUS and APO-UNSUS rats (n=7-8 per group). Samples were normalized against the housekeeping genes β-actin and Gapdh. **D.** Mean normalised mRNA expression in dorsomedial striatum of PND21 APO-SUS and APO-UNSUS rats (n=7-8 per group). Samples were normalized against the housekeeping genes β-Actin and Ywhaz. **E.** Mean normalised mRNA expression in striatum of PND28 APO-SUS and APO-UNSUS rats (n=8 per group). Samples were normalized against the housekeeping genes β-Actin and Cyc-A.

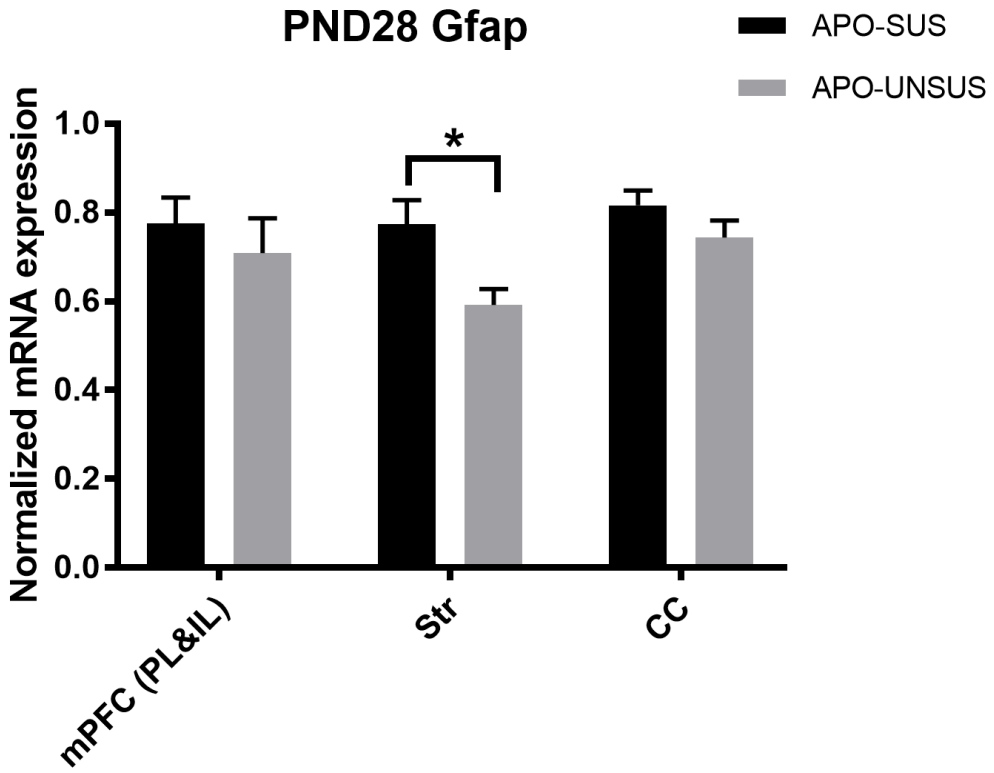

Supplemental Figure 5. mRNA expression of Gfap in the mPFC, striatum and corpus callosum of APO-SUS and APO-UNSUS rats at PND28

The bars represent the mean normalised mRNA expression of the astrocyte marker Gfap in the mPFC, striatum and corpus callosum of PND28 APO-SUS (black) and APO-UNSUS (grey) rats, along with error bars for the standard error of the mean. The asterisk (*) indicates statistically significant difference in gene expression between APO-SUS and APO-UNSUS, which was determined by the independent samples Student's t-test ($p \leq 0.05$, n=8 per group) after testing for outliers with the Grubbs test for outliers. mPFC samples were normalized against the housekeeping genes Gapdh and Ywhaz, striatum(Str) samples against β-Actin and Cyc-A and corpus callosum (CC) samples against Cyc-A and Ywhaz.

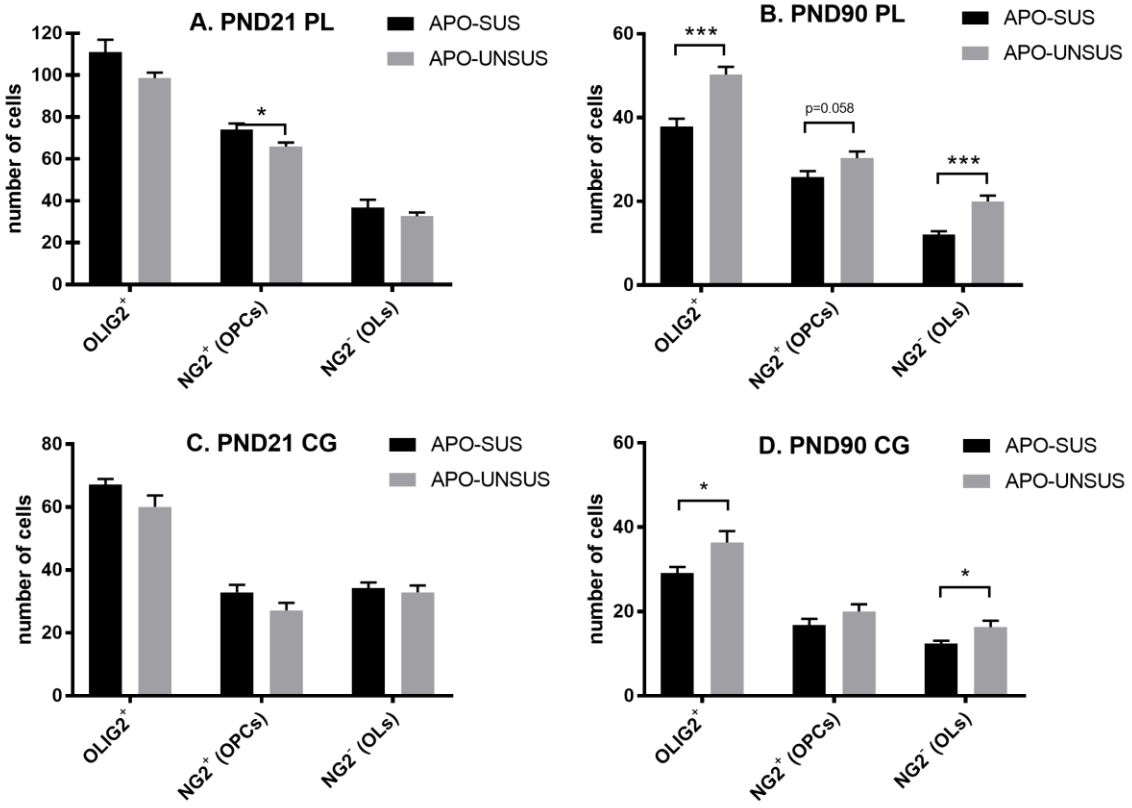

Supplemental Figure 6. OPC and OL density in the prelimbic and cingulate subregions of mPFC of APO-SUS and APO-UNSUS rats

Quantification of OPCs and OLs in the prelimbic (PL) and cingulate (CG) cortices of PND21 and PND90 APO-SUS and APO-UNSUS male rats. The bars represent the mean number of cells in APO-SUS (black) and APO-UNSUS (grey), along with error bars for the standard error of the mean. Asterisks (*) indicate statistically significant difference in cell density between APO-SUS and APO-UNSUS, which was determined by the independent samples Student's t-test after removal of the outliers by the Grubbs test for outliers (* $p \leq 0.05$, *** $p \leq 0.001$). The first set of bars in each graph displays the number of $OLIG2^+$ cells, which is translated to the total amount of OLs and OPCs. This number was split in two in the next two sets of bars with the help of NG2 staining. The middle set depicts the number of OPCs alone (cells that are $OLIG2^+$ and simultaneously $NG2^+$) and the last set of bars shows the number of OLs (cells that are $OLIG2^+$ but $NG2^-$). **A**. OPC and OL density in the prelimbic cortex of PND21 APO-SUS and APO-UNSUS (n=8 per group). **B**. OPC and OL density in the prelimbic cortex of PND90 APO-SUS and APO-UNSUS (n=7 per group). **C**. OPC and OL density in the cingulate cortex of PND21 APO-SUS and APO-UNSUS (n=8 per group). **D**. OPC and OL density in the cingulate cortex of PND90 APO-SUS and APO-UNSUS (n=7 per group).